BBA - Molecular Basis of Disease 1869 (2023) 166766

Contents lists available at ScienceDirect

BBA - Molecular Basis of Disease

journal homepage: www.elsevier.com/locate/bbadis

Functional and structural impact of 10 *ACADM* missense mutations on human medium chain acyl-Coa dehydrogenase

Catarina A. Madeira [a,1], Carolina Anselmo [a,1], João M. Costa [b], Cátia A. Bonito [c], Ricardo J. Ferreira [d], Daniel J.V.A. Santos [c,e], Ronald J. Wanders [f], João B. Vicente [b,*], Fátima V. Ventura [a,*], Paula Leandro [a,*]

[a] *Research Institute for Medicines, Faculty of Pharmacy, Universidade de Lisboa, Av. Prof. Gama Pinto, 1649-003 Lisboa, Portugal*
[b] *Instituto de Tecnologia Química e Biológica António Xavier, Universidade Nova de Lisboa, Av. da República, 2780-157 Oeiras, Portugal*
[c] *LAQV@REQUIMTE/Department of Chemistry and Biochemistry, Faculty of Sciences, University of Porto, Rua do Campo Alegre, 4169-007 Porto, Portugal*
[d] *Red Glead Discovery, Medicon Village, SE-223 81 Lund, Sweden*
[e] *Center for Research in Biosciences & Health Technologies (CBIOS), Universidade Lusófona de Humanidades e Tecnologias, Lisboa, Portugal*
[f] *Laboratory Genetic Metabolic Diseases, Department of Clinical Chemistry, Amsterdam University Medical Centers-University of Amsterdam, 1105 AZ Amsterdam, The Netherlands*

ARTICLE INFO

Keywords:
Inborn metabolic disorders
Medium chain acyl-CoA dehydrogenase deficiency
Disease-causing mutations
Protein misfolding
Flavin adenine dinucleotide
Electron transferring flavoprotein

ABSTRACT

Medium chain acyl-CoA dehydrogenase (MCAD) deficiency (MCADD) is associated with *ACADM* gene mutations, leading to an impaired function and/or structure of MCAD. Importantly, after import into the mitochondria, MCAD must incorporate a molecule of flavin adenine dinucleotide (FAD) per subunit and assemble into tetramers. However, the effect of MCAD amino acid substitutions on FAD incorporation has not been investigated. Herein, the commonest MCAD variant (p.K304E) and 11 additional rare variants (p.Y48C, p.R55G, p.A88P, p.Y133C, p.A140T, p.D143V, p.G224R, p.L238F, p.V264I, p.Y372N, and p.G377V) were functionally and structurally characterized. Half of the studied variants presented a FAD content <65 % compared to the wild-type. Most of them were recovered as tetramers, except the p.Y372N (mainly as dimers). No correlation was found between the levels of tetramers and FAD content. However, a correlation between FAD content and the cofactor's affinity, proteolytic stability, thermostability, and thermal inactivation was established. We showed that the studied amino acid changes in MCAD may alter the substrate chain-length dependence and the interaction with electron-transferring-flavoprotein (ETF) necessary for a proper functioning electron transfer thus adding additional layers of complexity to the pathological effect of *ACADM* missense mutations. Although the majority of the variant MCADs presented an impaired capacity to retain FAD during their synthesis, some of them were structurally rescued by cofactor supplementation, suggesting that in the mitochondrial environment the levels and activity of those variants may be dependent of FAD's availability thus contributing for the heterogeneity of the MCADD phenotype found in patients presenting the same genotype.

1. Introduction

Medium-chain acyl-CoA dehydrogenase (MCAD; EC 1.3.8.7) belongs to the family of acyl-CoA dehydrogenases (ACADs), which includes 11 mitochondrial flavoenzymes participating in different metabolic pathways [1,2]. The short (SCAD), medium (MCAD), long (LCAD), very long chain (VLCAD) and family member 9 (ACAD9) acyl-CoA dehydrogenases are involved in mitochondrial fatty acid β-oxidation (FAO), whereas the short-branched chain acyl-CoA (SBCAD), isovaleryl-CoA (IVDH), glutaryl-CoA (GCDH) and isobutyryl-CoA (IBDH) dehydrogenases participate in the amino acid catabolism. Two additional members are also involved in FAO namely the acyl-CoA dehydrogenase family members 10 (ACAD10) and 11 (ACAD11) [3]. ACAD10 has weak dehydrogenase activity against several long and branched-chain acyl-CoA substrates, while ACAD11, besides presenting a specificity towards docosanoyl-CoA (C22-CoA) and a lower activity against other long-

* Corresponding authors.
E-mail addresses: jvicente@itqb.unl.pt (J.B. Vicente), fatima.ventura@ff.ulisboa.pt (F.V. Ventura), aleandro@ff.ulisboa.pt (P. Leandro).
[1] These authors have contributed equally to this work and share first authorship.

https://doi.org/10.1016/j.bbadis.2023.166766
Received 6 February 2023; Received in revised form 10 May 2023; Accepted 23 May 2023
Available online 29 May 2023

chain fatty acid-CoA substrates, was found not only in mitochondria but also on cytoplasmatic vesicles and nuclei, at least in human skin fibroblasts [3]. VLCAD and ACAD9 assemble as homodimers whereas the remaining ACADs are homotetramers.

MCAD catalyses the first step in mitochondrial FAO (mFAO) which involves the α,β-dehydrogenation of acyl-CoAs of medium chain lengths including butyryl-CoA (C4-CoA), hexanoyl-CoA (C6-CoA), octanoyl-CoA (C8-CoA), decanoyl-CoA (C10-CoA), lauroyl-CoA (C12-CoA) and tetradecanoyl-CoA (C14-CoA), with a preference for C6- to C12-CoA substrates and a maximum catalytic efficiency for C8-CoA [2,4,5]. This enzyme is encoded by the *ACADM* nuclear gene and is synthesized in the cytosol as a polypeptide chain of 421 amino acids. Upon mitochondrial import, the mature functional protein is formed in the matrix through the cleavage of the N-terminal signal peptide (25 residues) [6]. The incorporation of flavin adenine dinucleotide (FAD) in the polypeptide chain promotes protein folding which is followed by the assembly into homotetramers (~176 kDa) as a result of dimerization of the homodimers [7–10]. Each mature monomer (396 residues; ~44 kDa) contains three structural domains: the N- and C-terminal α-domains (αND, α-helices A–F, residues 1 to 126; and αCD, α-helices G–K, residues 243 to 396; respectively) and an intermediary β-sheet domain (βD; β-strands 1–7; residues 129 to 233) [11]. Four α-helices of each monomer, as a pseudo four-helix bundle structure (α-helices G–I and K), form the core of the tetramer [7,11,12] with α-helices H and I of each monomer establishing contacts responsible for the protein's tetramerization. The homotetrameric MCAD presents four catalytic pockets where FAD binds noncovalently, acting as the cofactor, essential for the enzyme's function and structure [7,13]. Within the catalytic pocket, the terminal acyl chain of the substrate is buried between the αND and the αCD, while its 3′-phosphoadenosine moiety is located at the interface between the two monomers of a dimer and partially exposed to the solvent [7,11,12]. FAD establishes contacts with both subunits of a dimer. The flavin ring of FAD is positioned between the βD and αCD of a monomer and is aligned with the substrate acyl group and the protein's catalytic residue Glu376 [11] allowing the α,β dehydrogenation of the substrate to occur thereby producing the corresponding *trans*-2-enoyl-CoA and $FADH_2$ [14]. The adenosine moiety of the FAD interacts with the αCD of the neighbouring protein subunit within the dimer.

In the context of mitochondrial energy metabolism, the production of $FADH_2$, as catalysed by MCAD, has an important role as the subsequent re-oxidation to FAD by the electron-transferring flavoprotein (ETF) allows the establishment of electron flux towards the respiratory chain through the mitochondrial inner membrane ETF:ubiquinone oxidoreductase (ETF-QO) also referred to as ETF dehydrogenase (ETFDH) [13]. ETF is a mitochondrial matrix localized heterodimeric protein, composed of an α subunit (32 kDa; ETF-α) and β subunit (28 kDa; ETF-β), containing one FAD molecule (ETF-α) and one adenosine 5′- monophosphate (AMP; ETF-β) [15]. ETF acts as a mitochondrial electron transfer hub, since it accepts electrons not only from MCAD but also from the other ACADs and additional mitochondrial flavoenzymes involved in different metabolic pathways. The reducing equivalents obtained by ETF, are then transferred to the mitochondrial inner membrane enzyme ETF:QO, which in turn delivers the electrons to ubiquinone thereby feeding the respiratory chain [2,16,17] with reducing equivalents. In this perspective, the establishment of MCAD/ETF interactions is fundamental to maintain the FAO-Oxidative Phosphorylation communication. These MCAD/ETF interactions are mainly established through salt bridges and hydrogen bonds involving α-helices C and D of the αND of a MCAD monomer and the ETF-β recognition loop (Arg191 to Lys200) [18]. The FAD molecules of both proteins must be in close proximity (14 Å rule) in order to allow electron transfer to occur [19,20]. It has been suggested that the repositioning of the ETF-α will bring its FAD close to the neighbouring monomer of the MCAD dimer allowing electron transfer [18,21]. Conformational changes due to amino acid substitutions in MCAD sequence may directly or indirectly affect the ETF/MCAD recognition and/or interaction, further impairing the electron transfer from MCAD to ETF thus preventing electron flow and precluding MCAD $FADH_2$ re-oxidation back to FAD.

Mutations in the *ACADM* gene are responsible for MCAD deficiency (MCADD; OMIM #201450, ORPHA42), an autosomal recessive inborn metabolic disorder (IMD) and the most common disorder of the mFAO pathway [13,22]. MCADD is not only clinically heterogeneous, but the same is true for the corresponding biochemical and mutational profiles, which complicate proper diagnosis, and treatment [23]. Currently, MCADD is included in newborn screening (NBS) programmes in many countries [24,25], contributing to reduce the associated morbidity and mortality. MCADD patients are mostly asymptomatic but episodes of metabolic stress (*e.g.* prolonged fasting, intense exercise or illness with fever episodes) may lead to hypoketotic hypoglycemia, elevated liver enzymes and hepatosteatosis, encephalopathy, coma, and death [13]. The prevalence of MCADD has been calculated to be ≈1:15,000 in Caucasians, with other populations displaying lower frequencies [24,26]. Epidemiological data also revealed that MCADD is the most frequent IMD in many countries [27–29], mainly due to the high frequency of the c. 985G>A *ACADM* gene mutation in those populations. To date, 432 different *ACADM* gene variations were identified (ClinVar, National Center for Biotechnology Information (https://ncbi.nlm.nih.gov/clinvar/); accessed 28 April 2023), from which 68 are classified as pathogenic, 82 as likely pathogenic and 165 are grouped as uncertain/conflicting. Nevertheless from these putative 315 disease-causing *ACADM* gene variations the large majority is classified as missense mutations (≈69 %) leading to an impaired function and/or structure of MCAD [7,30–34]. Therefore, MCADD is considered a conformational disorder with associated loss-of-function [32,34]. Presently, pharmacological therapies for MCADD are not available. Treatment strategies mainly involve dietary control of lipids intake and avoiding fasting [35], but many patients still present life-threatening decompensation episodes, with reports of serious metabolic crisis and sudden death among controlled individuals [26,30,36]. This reflects the urgency of addressing the unmet medical needs of MCADD patients through the research and development of therapeutic strategies to minimize the potential MCADD associated morbidity and mortality.

Being considered a conformational disorder, MCADD is a potential candidate for the treatment with pharmacological chaperones, which are small compounds able to promote conformational stabilization, thereby avoiding the intracellular degradation of the protein and rescuing enzyme function. Although this approach has never been investigated in MCADD management, treatment with pharmacological chaperones has been already implemented [37] or investigated for some IMD [38–40].

The c.985A>G transition is the most common *ACADM* mutation, identified in homozygosity in 50–80 % of MCADD patients and in compound heterozygosity with rare mutant alleles in about 20 % of the MCADD population [27,41]. At the protein level, the c.985A>G *ACADM* mutation results in the substitution of a lysine (K) by a glutamate (E) at position 304 (p.K304E) of mature MCAD (p.K329E in the precursor protein containing the 25 amino acids of the mitochondrial signal peptide). This variant has been extensively characterized at the biochemical and structural levels [30–32,42,43]. However, until now, only a limited number of the less frequently identified MCAD variants have been studied.

In this work, we studied the p.K304E variant and a group of 11 rare MCAD variants (amino acid residues numbering corresponding to the mature protein), identified in MCADD patients in Portugal and in The Netherlands [27,44–46] (Table S1), which were selected by their localization in the three protein domains namely αND (p.Y48C, p.R55G and p.A88P), βD (p.Y133C, p.A140T, p.D143V and p.G224R), and αCD (p.L238F, p.V264I, p.Y372N and p.G377V). Due to the relevance of the cofactor FAD, not only for the enzymatic reaction catalysed by MCAD but also for its protein structure, we studied the FAD content and binding capacity as well as its role on the conformational stability of MCAD variants. To understand if amino acid changes in the MCAD sequence

can interfere with its interaction with ETF, we also studied the enzyme's activity using the artificial and natural electron acceptors. The obtained data will allow not only to understand the molecular basis of MCADD but also to devise small molecules to be used as stabilizers of the variant proteins (pharmacological chaperones) which qualify as future medicines for the treatment of this rare genetic metabolic disease.

2. Material and methods

2.1. Expression and purification of recombinant wild-type and variant MCAD

The nucleotide numbering is based on the GenBank RefSeq M16827.1. The *ACADM* DNA mutation numbering system is based on the cDNA, with +1 corresponding to the A of the ATG translation initiation codon in the reference sequence. *ACADM* gene is translated as a full-length precursor protein containing the N-terminal mitochondrial signalling peptide (25 amino acid residues). In this work amino acid residues were numbered according to the sequence of the mature protein with Lys1 corresponding to Lys26 in the precursor protein.

The wild-type (WT) MCAD cDNA (kindly provided by N. Gregersen, DK), encoding the mature protein, was cloned into the *Nde*I and *Hind*III sites of the pET28a(+) expression vector in frame with a C-terminal 6×Histidine (6×His) tag, as previously reported [43]. The *ACADM* gene mutation c.985A>G (p.K304E) was obtained as previously described [43]. The c.218A>G (p.Y48C), c.238A>G (p.R55G), c.337G>C (p.A88P), c.473A>G (p.Y133C) c.493G>A (p.A140T), c.503A>T (p.D143V), c.745G>A (p.G224R), c.789A>C (p.L238F), c.865G>A (p.V264I), c.1189T>A (p.Y372N) and c.1205G>T (p.G377V) *ACADM* gene mutations were generated by site-directed mutagenesis using the XL Quick Change II system (Agilent, Santa Clara, CA, USA) and the mutagenic oligonucleotides described in Table S2. The obtained constructs were sequenced in both directions to verify the introduction of the desired mutations and exclude additional mutational events.

The WT and variant forms of MCAD were expressed in *Escherichia (E.). coli* BL21 (DE3) and purified by immobilized metal affinity chromatography (IMAC) as described previously [43] with some minor modifications. Briefly, bacterial cells transformed with the expression constructs were grown in Luria-Bertani (LB) medium, supplemented with kanamycin (50 μg·mL^{-1}), at 37 °C, 140 rpm, until an OD_{600nm} of 0.6–0.8. Protein expression was then induced by adding isopropyl β-D-1-thiogalactopyranoside (IPTG, 1 mM). After incubation for 21 h at 27 °C, 140 rpm, cells were harvested (2057 g, 10 min, 4 °C), resuspended in buffer A (20 mM potassium phosphate buffer, pH 7.4, 500 mM NaCl) containing 1 mg·mL^{-1} lysozyme, 1 mM phenylmethylsulfonyl fluoride (PMSF), 0.5 μg·mL^{-1} DNase and 0.1 mg·mL^{-1} FAD. Cells were lysed by sonication and the soluble fraction was obtained after centrifugation at 12,857*g* for 40 min, 4 °C. The soluble proteins were purified by IMAC (Ni-NTA agarose; Qiagen; Hilden, Germany) using buffer A and an imidazole gradient (20–250 mM) as previously described [43]. The IMAC fractions containing the recombinant MCAD proteins were pooled, concentrated to a final volume of 2.5 mL using a 30 K MWCO protein concentrator (Amicon® Ultra – 15; Millipore, Burlington, MA, USA) and used for size exclusion chromatography (SEC). The MCAD tetramers were further purified on a Hiload™ 16/60 Superdex™ 200 prep grade column (GE Healthcare; Chicago, IL, USA), using the SEC buffer (20 mM potassium phosphate buffer, pH 7.4, 200 mM NaCl) and a flow rate of 0.7 mL·min^{-1} in an AKTA®primeplus system (GE Healthcare) equipped with a UV detector (λ 280 nm) and a fraction collector.

The purified tetramers were quantified using the Bio-Rad Protein assay (Bio-Rad; Hercules, USA) and bovine serum albumin (BSA) as standard. To assess purity the obtained proteins (1 μg) were loaded into a 12.5 % polyacrylamide gel (Criterion TGX 12 %, Bio-Rad) and visualized using NzyBlue Safe (NZYTech; Lisboa, Portugal). The UV–Vis spectrum (λ 250–600 nm) of recombinant MCAD (WT and variants), at 130 μg·mL^{-1} in SEC buffer, was monitored on a Shimadzu UV-VIS spectrophotometer (Shimadzu Corporation, Japan) to evaluate FAD incorporation by either analyzing the $Abs_{280\ nm}/Abs_{450\ nm}$ ratio and quantifying the FAD content (ε_{450nm} = 14.5 mM^{-1}·cm^{-1}) [5,47]. The purified recombinant MCAD tetramers were stored at −80 °C in 20 % of glycerol.

2.2. Expression and purification of recombinant ETF

For the expression of the ETF protein (ETF-α and ETF-β) a bicistronic expression system was used produced by NZYTech (Supplementary Fig. S1), employing the design described in Bross et al. [48]. The cDNAs of the WT ETF-β (GenBank: X71129.1) and ETF-α (GenBank: J04058) were synthesized (codon optimized for expression in *E. coli*) and cloned into the pHTP1 expression vector (Nzytech), each being under the control of an individual T7 promoter and T7 terminator. A 6×His tag is at the N-terminus of the ETF-β subunit.

Recombinant ETF was expressed in *E. coli* BL21 (DE3) and purified by IMAC following the protocol described in Augustin et al. [49] with some minor modifications. Briefly, cells were grown in TB medium supplemented with kanamycin (50 μg·mL^{-1}) at 37 °C, 140 rpm, until an $OD_{600\ nm} \geq 1.5$. The protein expression was induced using 0.5 mM IPTG. After incubation for 4 h, at 37 °C, 140 rpm, cells were collected by centrifugation (10 min; 2057*g*; 4 °C). Cells were further resuspended in buffer A, containing lysozyme (1 mg·mL^{-1}), PMSF (1 mM), DNase (0.5 μg·mL^{-1}) and FAD (0.1 mg·mL^{-1}), and lysed by sonication, as above. The recombinant proteins were IMAC purified using an imidazole gradient (20 to 300 mM) consisting of three washing steps (20 mM, 40 mM and 75 mM) and elution with 300 mM imidazole. A PD-10 desalting column was used to eliminate the presence of imidazole on eluted fractions and to exchange to buffer B (50 mM Na-Hepes, pH 7.0, 200 mM NaCl). The ETF protein was quantified (BioRad protein assay), analysed by SDS-PAGE as above and stored in 10 % glycerol at −80 °C. When necessary, the protein aliquots were concentrated using a 10 K MWCO protein concentrator (Amicon® Ultra – 15) at 3000*g* at 4 °C.

2.3. FAD binding affinity assays

The relative affinity of MCAD variants for the FAD cofactor was assessed by differential scanning fluorimetry (DSF) assays. The DSF assays were performed in the absence and presence of increasing FAD concentrations (2.5–80 μM range [50–52] in SEC buffer, in a reaction volume of 50 μL containing recombinant MCAD proteins (5 μg) and SYPRO Orange at a final concentration of 2.5-fold (5000-fold stock solution from Invitrogen, Carlsbad, CA, USA). Assays were run in a Real-Time PCR system (C1000 Touch® Thermal Cycler; Bio-Rad) with fluorescence acquisition in the FRET channel (10 min incubation at 20 °C followed by a 1 °C·min^{-1} linear temperature gradient up to 90 °C), as previously described [43]. Data were fitted to a sigmoidal dose-response equation using GraphPad Prism, thus allowing the determination of the melting temperature (T_m). The difference between the T_m value at a given FAD concentration and the T_m in the absence of FAD was defined as ΔT_m. To calculate the FAD binding affinity (k_B), the ΔT_m values were plotted as a function of FAD concentration and the data were fitted with a one site-specific binding equation and the apparent binding affinity constants (k_b) were determined.

2.4. Enzyme activity of purified MCADs

The specific enzyme activity of purified recombinant MCAD proteins was determined using either phenazine methosulfate (PMS) and the terminal 2,6-dichlorophenolindophenol (DCPIP) as artificial electron carriers or the natural electron carrier ETF together with DCPIP [53,54]. The concentration of acyl-CoA substrates and DCPIP were always adjusted by using $\varepsilon_{260\ nm}$ 15.4 mM^{-1}·cm^{-1} and $\varepsilon_{600\ nm}$ 21 mM^{-1}·cm^{-1}, respectively [5]. The enzyme reactions were performed in SEC buffer, in a final volume of 180 μL containing 2.5 μg of purified MCAD (WT or

variants), 1.5 mM PMS or 20 μg of recombinant ETF and 48 μM DCPIP. The reaction was started by adding 20 μL of the corresponding acyl-CoA substrate (C6-CoA, C8-CoA, C10-CoA and C12-CoA; Sigma-Aldrich; St. Louis, MO, USA) at a final concentration of 33 μM. The reaction was followed by measuring the DCPIP absorption decrease at $\lambda_{600\ nm}$ for 200 s, at 25 °C, on a ZENYTH 3100 microplate reader (Anthos Labtec, Salzburg, Austria), equipped with a 595 ± 8 nm filter. Specific enzyme activities were expressed as μmol of DCPIP reduced per min per mg of MCAD protein (μmol DCPIP·min^{-1}·mg^{-1}).

Kinetic assays were performed using C8-CoA concentrations from 1 to 100 μM. The steady-state kinetic data were analysed by non-linear regression analysis using GraphPad Prism (La Jolla, CA, USA) and the Michaelis-Menten equation.

Thermal inactivation profiles were obtained for the purified MCAD tetramers by pre-incubating protein aliquots (5 μg) at different temperatures (25–70 °C) for 10 min and chilling them on ice (10 min) prior to determining enzymatic activity using C8-CoA as the substrate and the redox pair PMS/DCPIP as described above. The mid-point of thermal inactivation ($T_{1/2}$), which indicates the temperature at which the protein presents 50 % residual activity was determined by non-linear regression analysis.

2.5. Far-UV circular dichroism

Far-UV circular dichroism (CD) was employed to analyse the secondary structure content of MCAD variants in comparison with the WT protein. The far-UV CD experiments were carried out in a Jasco J-815 spectropolarimeter (Easton, MD, USA) equipped with a Jasco CDF-426S Peltier temperature controller. Protein samples were diluted to 0.15 mg·mL^{-1} in 20 mM potassium phosphate (KPi) buffer, pH 7.4 and transferred to a 0.1 cm path quartz cuvette. The spectra were acquired at 20 °C, resulting from four accumulations under the following conditions: 50 nm·min^{-1} scanning speed; data pitch 0.5 nm; data integration time (DIT) 2 s; bandwidth 2 nm; N_2 flow 8 L·min^{-1}. The experimental setup for thermal denaturation profiles was: λ = 222 nm; temperature range 20–90 °C; 1 °C·min^{-1} temperature gradient; data pitch 0.5 °C; DIT 1 s; bandwidth 2 nm; N_2 flow 4 L·min^{-1}. The thermal denaturation curves were analysed according to a two-state model and the T_m values were determined as the inflexion points from the fitted sigmoidal thermal denaturation curves.

2.6. Thermal stability assays

In addition to far-UV CD-monitored thermal denaturation curves, dye-free differential scanning fluorimetry (dfDSF) was employed to probe the thermal denaturation of MCAD variants following different molecular events. The dfDSF assays to analyse FAD-associated fluorescence ($dfDSF_{FAD}$) were performed in an Applied Biosystems QuantStudio 7 Flex RT-PCR, monitoring the flavin fluorescence (λ_{exc} 470 nm, λ_{em} 558 nm) as a function of temperature. The dfDSF assays analyzing intrinsic tryptophan fluorescence ($dfDSF_{ITF}$; λ_{exc} 275 nm, λ_{em} 330 nm), to probe global protein thermal denaturation, were performed in a nanoTemper Prometheus NT.48 nanoDSF. All variants were analysed at 0.5–0.6 mg·mL^{-1} in SEC buffer. In both approaches, thermal melting experiments were done by increasing the temperature between 20 and 90 °C at a linear temperature rate of 1 °C·min^{-1}. The $dfDSF_{FAD}$ assay allowed the estimation of the midpoint of the FAD-associated fluorescence as a function of temperature ($T_{50(FAD)}$). The thermal denaturation curves obtained by $dfDSF_{ITF}$ were best fitted with a sum of two sigmoidal curves, accounting for two transitions, allowing determination of Frac (difference between fitted T_{m1} and T_{m2} values).

To evaluate the kinetics of the thermal denaturation of recombinant MCAD (WT and variants), an isothermal denaturation fluorimetry (ITDF) assay was performed. In this assay, the C1000 Touch® Thermal Cycler (Bio-Rad) was used to measure the fluorescence, at a fixed temperature (42 °C), over time (150 min). The reaction mixtures were prepared as in the flavin binding affinity assays. One-phase or two-phase dissociation functions were used to fit the data and to obtain the half-lives, using GraphPad Prism. The denaturation rate (k) was calculated from the slope at the lowest half-life obtained for each temperature studied [55].

2.7. Limited proteolysis

Limited proteolysis by trypsin assays was performed in SEC buffer, at 37 °C, and in a final volume of 210 μL containing 42 μg of purified recombinant MCAD (WT or variants), 0.12 μg trypsin (1:25 (m:m) trypsin: protein ratio) and in the absence or presence of 80 μM FAD. At different time points (0–120 min), aliquots (15 μL) of the reaction were collected and the proteolysis was stopped by the addition of soybean trypsin inhibitor (1:1.5, m:m) protease:inhibitor ratio). The samples were analysed by SDS-PAGE (12.5 %) and the full-length protein was quantified by densitometry using Image J® 1.52K (NIH, USA). The data obtained were fitted to a one-phase exponential decay equation (GraphPad Prism) to determine the plateaus of degradation (% of full-length protein at infinite time) as a measure of the full-length protein resistant to proteolysis ($FL_{Plateau}$) [43].

2.8. Statistical and in silico analysis

The data obtained from independent experiments ($N \geq 3$) are presented as the mean ± standard deviation ($\overline{X} \pm S.D.$). Statistical significance (P) was determined by the Student's paired t-test. A $P < 0.05$ was considered significant. The correlation between data was determined with the Pearson Correlation assay using GraphPad Prism to obtain the correlation coefficient (r) and P ($P < 0.05$ was set as the significant criterion).

The effect of the introduced substitutions on the thermodynamic stability and protein conformation of the protein was estimated using the Site Directed Mutator (SDM) server (http://marid.bioc.cam.ac.uk/sdm2) [56] and the coordinates of MCAD/ETF complex (PDB ID: 1T9G). The coordinates of pig (*sus scrofa*) MCAD structure (PDB ID: 1UDY) were loaded into UCSF Chimera [57] and the amino acid changes were obtained with the structure editing tool of Chimera. The most probable rotamer of the substituting amino acid was selected and the resulting steric hindrances were analysed. Structural images were produced using UCSF Chimera.

3. Results

3.1. Production, oligomeric profile and secondary structure of recombinant MCAD variants

In this work cell lysis was always performed in the presence of 0.1 mg·mL^{-1} FAD, to prevent the cofactor loss during the harsh sonication procedure. The need for cofactor supplementation during protein expression was also assessed. As no difference in protein yields was observed, protein expression was always performed without FAD addition to the culture medium (data not shown). From the 12 variant proteins analysed, only two (p.A88P and p.L238F) presented very low levels in the soluble fraction of *E. coli* lysates preventing their further purification, and therefore were excluded from this study. After IMAC purification the remaining 10 variants were recovered in different yields varying from 0.38 ± 0.28 (p.Y48C) to 1.16 ± 0.42 mg (p.R55G) per litre of cell culture (Table S3).

The recombinant MCADs (WT and variants) obtained by IMAC were further purified by SEC to isolate the biologically active tetramers. Size-exclusion chromatography was also used to monitor the oligomeric profile of the recombinant MCAD variants in comparison with the oligomeric profile of the recombinant WT protein. As shown in Fig. 1, from the 10 variants studied only three presented a relative percentage

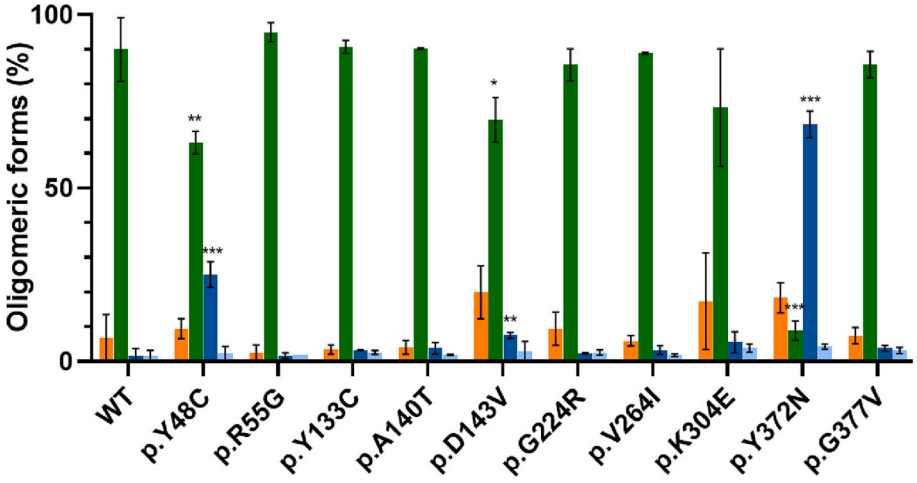

Fig. 1. Oligomeric profile of recombinant wild-type (WT) medium chain acyl-CoA dehydrogenase (MCAD) and variants after purification by immobilized metal affinity chromatography. The relative percentage of each oligomeric form corresponds to the ratio between the intensity of the peaks observed in the size exclusion chromatography (SEC) chromatograms for that oligomeric form and the totality of the oligomeric forms analysed. (■) High molecular weight forms (HWM), >400 kDa); (■) Tetramers, ≈160 kDa; (■) Dimers, ≈80 kDa; and (■) Monomers, ≈40 kDa. Values represent $\overline{X} \pm S.D.$ of at least three independent expression and purification assays, except for the p.R55G ($N = 2$). P (*<0.05, **<0.005, and ***<0.0001) was calculated by comparing MCAD variant values with the WT.

of tetramers (MM ≈ 160 kDa) lower than that found for the WT protein (89.9 ± 9.2 %), namely the p.Y48C (63.1 ± 3.3 %, $P < 0.005$), p.D143V (69.7 ± 6.4 %, $P < 0.05$) and p.Y372N (9.0 ± 2.8 %, $P < 0.0001$). For the p.Y48C and p.Y372N the lower level of tetramers was mainly due to a higher percentage of dimers (MM ≈ 80 kDa), with the p.Y372N being mostly recovered in this form (68.4 ± 3.9 %, $P < 0.0001$; WT: 1.7 ± 1.9 %). When compared with WT (6.7 ± 6.8 %), a higher level of high molecular forms (HMW; MM > 400 kDa) were also observed for the p.D143V (19.9 ± 7.6 %, $P < 0.05$) and p.Y372N (18.4 ± 4.3 %, $P < 0.05$). None of the recombinant MCAD proteins presented significant levels of monomers (MM ≈ 40 kDa), which ranged from 1.6 % (WT) to 4.3 % (p.Y372N), nor were purified mainly in their HMW form (Fig. 1). As the low levels of p.Y372N tetramers (8.9 ± 2.8 %) precluded their use for additional assays, all further studies with this variant were performed with the isolated dimers.

Far-UV CD was employed to analyse the effect of the studied amino acid substitutions resulting from *ACADM* missense mutations on the secondary structure of the respective MCAD variants. As observed in Fig. 2, the Far-UV CD spectrum of WT MCAD is dominated by two major bands centered at ~225 nm and ~210 nm. The spectra recorded for the studied variants display essentially the same spectral features, with a similar ratio between the intensity of the two bands as compared to WT MCAD.

3.2. Flavinylation status and apparent FAD binding affinity of the recombinant MCADs

The FAD content of the WT and variant recombinant MCADs is depicted in Table 1. The observed FAD:WT molar ratio was 0.88/subunit and the Abs_{280}/Abs_{450} was 5.3, in line with the values reported in the literature for the recombinant WT MCAD [5] and indicating a high FAD content with almost full occupancy (Abs_{280}/Abs_{450} 5.2–5.5) [58] in the produced recombinant WT MCAD. The data obtained for the studied variants suggest that five out of the ten proteins (p.Y48C, p.Y133C, p.A140T, p.D143V and p.Y372N) did not incorporate FAD as efficiently as the WT as low levels of FAD content/subunit (<0.56) and high ratios of Abs_{280}/Abs_{450} (>8.0) were observed. Moreover, among these variants, the lowest content (<33 % of WT) was determined for the p.A140T and p.Y372N variants, with the p.D143V variant showing virtually no FAD content. Interestingly, the p.Y372N and p.D143V variants also presented a low percentage of tetramers (Fig. 1). Considering these data the studied variants were grouped according to the degree of FAD incorporation as Group I (FAD content <67 % of WT; p.Y48C, p.Y133C, p.A140T, p.D143V and p.Y372N) and Group II (FAD content >78 % of WT; p.R55G, p.G224R, p.V264I, p.K304E and p.G377V).

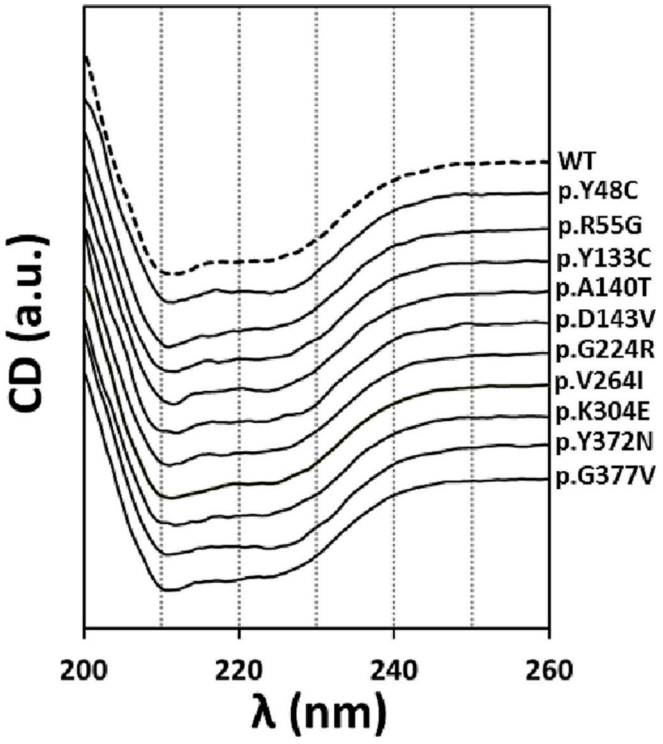

Fig. 2. Impact of amino acid substitutions on the secondary structure of recombinant medium chain acyl-CoA dehydrogenase (MCAD) variants probed by Far-UV circular dichroism (Far-UV CD) spectropolarimetry by comparison with the secondary structure of the recombinant wild-type (WT) MCAD. The Far-UV CD spectra were collected in a 0.1 cm light path cuvette at 20 °C. Variants and WT MCAD were at 0.15 mg·mL^{-1}, in 20 mM KPi, pH 7.4. The spectra were offset for presentation purposes. (a.u.) Arbitrary units.

In line with the observed FAD content in the purified enzymes, the MCAD variants with lower FAD content presented higher apparent binding affinities (k_B), ranging from 13.1 ± 2.2 (p.V264I) to 44.0 ± 12.2 μM (p.A140T) (Table 1 and Fig. S2), to be compared with WT MCAD (7.4 ± 1.3 μM). Conversely, the p.R55G, p.G224R, and p.K304E variants, presenting similar FAD content to the WT, also showed k_B in the same range. Out of this trend, and when compared to the WT, the p.

Table 1
FAD content determined by UV–Vis spectrophotometry, and apparent FAD binding constant (k_B) determined by differential scanning fluorimetry (DSF), of recombinant wild-type (WT) and variant MCAD tetramers (Group I: low FAD content; Group II: FAD content similar to WT).

		FAD content/subunit (molar ratio)	Abs_{280}/Abs_{450}	k_B FAD (μM)
WT		0.88	5.3	7.4 ± 1.3
	p.Y48C	0.56	8.0	19.8 ± 9.0
	p.Y133C	0.48	9.2	37.4 ± 1.9***
Group I	p.A140T	0.32	13.4	44.0 ± 12.2**
	p.D143V	n.d.	–	–[b]
	p.Y372N[a]	0.23	19.7	–[b]
	p.R55G	0.77	5.9	6.7 ± 0.6
	p.G224R	0.87	5.1	8.2 ± 0.9
Group II	p.V264I	0.77	5.8	13.1 ± 2.2*
	p.K304E	0.74	6.0	8.0 ± 1.3
	p.G377V	0.75	5.3	4.4 ± 0.8*

Notes: MCAD variants were grouped according to the FAD content being lower (Group I) or similar to the WT (Group II); (n.d.) Not detected. The FAD content was determined using the Abs_{450nm} and ε_{450nm} of 14.5 $mM^{-1}.cm^{-1}$. K_B values represent $\overline{X} \pm S.D.$ of at least three independent assays. Statistical significance was determined using the Multiple *t*-test and comparing the variant forms to the WT MCAD (*$P < 0.05$; **$P < 0.01$; ***$P < 0.0001$).

[a] Assays were performed with the dimers.

[b] For variants with very low FAD binding it was not possible to accurately determine the k_B.

V264I and p.G377V variants, for which a FAD content of 0.8 was determined (WT = 0.9), showed lower (k_B 13.1 ± 2.2 μM) and higher affinity (k_B 4.4 ± 0.8 μM) for the cofactor, respectively.

3.3. Catalytic properties of recombinant MCAD tetramers

The chain length specificity of the WT and variant MCAD tetramers catalytic activity was determined using 33 μM of substrates and the PMS/DCPIP assay. As shown in Fig. 3A, under these conditions, the WT MCAD presented the highest specific enzyme activity for C6-CoA (1.50 ± 0.12 μmol DCPIP·min^{-1}·mg^{-1}), followed by C8-CoA (1.20 ± 0.05 μmol DCPIP·min^{-1}·mg^{-1}), C10-CoA (1.10 ± 0.02 μmol DCPIP·min^{-1}·mg^{-1}) and C12-CoA (0.97 ± 0.05 μmol DCPIP·min^{-1}·mg^{-1}). The chain-length specificity and the specific activity of WT MCAD are in line with those obtained by other authors [4,42,59]. A similar chain-length dependency was observed for the majority of the studied recombinant MCAD variants (C6 > C8 > C10 > C12). Out of this trend, both p.R55G and p.Y133C variants presented the lowest activity in the presence of C8-CoA namely 0.96 ± 0.06 and 0.19 ± 0.01 μmol DCPIP·min^{-1}·mg^{-1}, respectively (Fig. 3A), with the latter showing maximum activity for the C12-CoA substrate (0.56 ± 0.04 μmol DCPIP·min^{-1}·mg^{-1}). For the MCAD variants with the lowest enzyme activities (p.D143V, pY372N and p.G377V) highest responses were obtained towards the C10-CoA substrate.

When compared with the WT recombinant MCAD (Fig. 3A and Supplementary Fig. S3), all the studied variants presented lower residual enzyme activities for the tested acyl-CoA substrates, except the p.R55G variant which only showed statistically significant differences towards the C8-CoA (Fig. 3A and B) and the p.V264I variant that did not present a statistically significant difference only towards the C8-CoA (relative enzyme activity: 98 ± 8 %; $P > 0.05$). Focusing on the activity towards the C8-CoA substrate, for which a maximum catalytic efficiency is described for MCAD [2,4,5] and in the data obtained in the PMS/DCPIP assay (Fig. 3A and B) significant decreases were observed for the residual activity of the recombinant variants p.Y48C (44 ± 10 %, $P < 0.005$), p.R55G (69 ± 1 %, $P < 0.005$), p.Y133C (16 ± 1 %; $P < 0.0001$), p.A140T (48 ± 1 %; $P < 0.0001$), p.G224R (46 ± 2 %, $P < 0.0001$), and p.K304E (74 ± 4 %, $P < 0.005$). The p.D143V, and p.G377V were the variants that showed the lowest residual enzyme activities (0.4 and 1 %, respectively). As expected, when compared to the WT tetramers, the p.Y372N dimers showed only 0.6 ± 0.3 % of residual enzyme activity.

In line with data described in the literature [5], when comparing the catalytic activity of the WT recombinant MCAD towards C8-CoA using the two electron acceptor pairs (Supplementary Fig. S3D and Fig. 3B) a lower activity (0.25 ± 0.02 μmol DCPIP·min^{-1}·mg^{-1}) was found when assayed with the ETF/DCPIP (PMS/DCPIP: 1.20 ± 0.05 μmol DCPIP·min^{-1}·mg^{-1}). The same trend was obtained for all the studied variants (Fig. S3D). The relative enzyme activity of the variants using the two different assays was then compared (Fig. 3B). The analysis of the residual activity obtained for the C8-CoA substrate using the two different assays (PMS/DCPIP and ETF/DCPIP; Fig. 3B) showed three different results among the recombinant MCAD variants studied: (i) same level of response between assays (for p.Y48C, p.A140T, p.D143V, p.V264I and p.G377V variants); (ii) higher level of response with PMS/DCPIP assay (for p.R55G, p.G224R and p.K304E variants; 31 %, 40 % and 20 % decrease, respectively) and (iii) higher level of response with the ETF/DCPIP assay (for p.Y133C and p.Y372N variants; 24 % and 5 % increase, respectively). In line with the data obtained with the PMS/DCPIP assay, the p.D143V and p.G377V were the variants presenting the lowest catalytic activity towards the C8-CoA substrate (not detected and 2.0 ± 0.1 % residual activity, respectively) also with the ETF/DCPIP assay. The p.Y372N dimers also presented a low residual enzyme activity with C8-CoA in the ETF/DCPIP assay (5.1 ± 0.1 % of the WT tetramers) that, however, was 5 % higher than the value obtained with the PMS/DCPIP assay.

The determination of the steady-state kinetic parameters of the recombinant WT and MCAD variants (Table 2; Fig. S4) revealed that the majority of the MCAD variants presented a V_{max} lower than the WT (1.57 ± 0.01 μmol DCPIP·min^{-1}·mg^{-1}) ranging from 0.21 ± 0.04 μmol DCPIP·min^{-1}·mg^{-1} (p.Y133C) to 1.25 ± 0.06 μmol DCPIP·min^{-1}·mg^{-1} (p.K304E). The p.V264I and the p.R55G variants presented a higher V_{max} than the WT (2.04 ± 0.05 μmol DCPIP·min^{-1}·mg^{-1} and 1.83 ± 0.09 μmol DCPIP·min^{-1}·mg^{-1}, respectively), although no statistically significant difference was observed for p.R55G. As for the affinity towards the C8-CoA substrate (K_M), when compared to the WT (13.2 ± 1.9 μM) the variants presenting a higher (p.V264I) or similar (p.R55G) V_{max}, showed higher K_M values for C8-CoA (lower affinity), namely 25.1 ± 2.4 μM (p.V264I; $P < 0.01$) and 26.2 ± 2.4 μM (p.R55G; $P < 0.005$), respectively. The higher K_M observed for the p.K304E variant (15.3 ± 2.4 μM) was not statistically significant when compared to the WT MCAD. Importantly, regarding the catalytic efficiency (*i.e.* K_M/V_{max}), five out of the seven variants, presented a catalytic efficiency lower than the value determined for the WT (9.7 ± 1.2 $μM^{-1}$·min^{-1}) ranging from 4.2 ± 2.3 $μM^{-1}$·min^{-1} (p.Y133C) to 7.0 ± 0.7 $μM^{-1}$·min^{-1} (p.G224R). For the remaining two variants (p.Y48C and p.A140T) the catalytic efficiencies (p.Y48C: 10.6 ± 3.9 $μM^{-1}$·min^{-1} and p.A140T: 8.8 ± 1.8 $μM^{-1}$·min^{-1}) were not statistically significantly different from the values found for the WT recombinant MCAD. The low enzymatic activity of the p.D143V, p.Y372N and p.G377V variants prohibited the study of their kinetic parameters.

3.4. Effect of amino acid changes on MCAD thermal and conformational stability

The impact of the missense *ACADM* mutations herein investigated on the MCAD's protein thermal stability was monitored by far-UV CD and dfDSF. In far-UV CD thermal denaturation experiments, protein unfolding was followed at 222 nm as a representative wavelength for α-helical structure loss (Fig. S5). The data were fitted according to a two-state model, allowing to estimate apparent T_m values for all variants (Table 3). Seven (p.Y48C, p.Y133C, p.A140T, p.D143V, p.V264I, p.K304E and p.Y372N) out of the ten variants studied presented T_m values >2.0 °C lower than the WT MCAD ($\Delta T_m > -2.0$ °C). The only variant

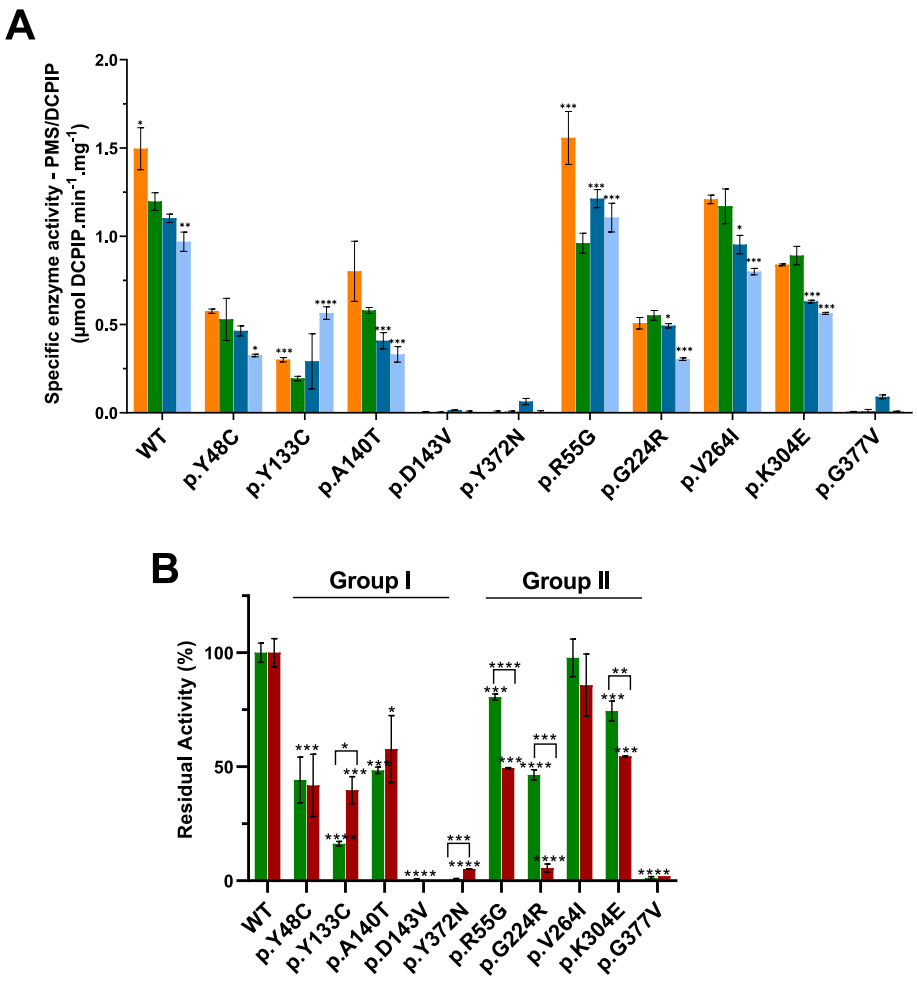

Fig. 3. Substrate chain-length dependence of the catalytic activity of wild-type (WT) and variant human medium chain acyl-CoA dehydrogenase (MCAD) tetramers. (A) The catalytic activity was determined using the PMS/DCPIP assay for the C6-CoA (■), C8-CoA (■),C10-CoA (■) and C12-CoA (■) substrates (33 μM); In B the assay was performed using the C8-CoA substrate and the PMS/DCPIP (■) and ETF/DCPIP (■) reaction. Data represent $\overline{X} \pm S.D.$ of at least three independent expression and purification assays, each analysed in triplicate. *P* values (*<0.05, **<0.01, ***<0.005 and ***<0.0001) were calculated by comparing the C6-, C10- and C12-CoA with the C8-CoA in A. In B the *P* calculated by comparing the PMS/DCPIP and ETF/DCPIP assays is also shown. The data for the p.Y372N variant were obtained using the dimeric forms. Group I: low FAD content; Group II: FAD content similar to WT.

with an apparent higher melting temperature than WT MCAD was the p.G377V variant.

The dye-free differential scanning fluorimetry (dfDSF) experiments were employed to probe the thermal denaturation of the recombinant MCAD variants following different molecular events. Monitoring the flavin fluorescence ($dfDSF_{FAD}$; Fig. S6 and orange lines in Fig. S7A–C) enabled probing changes in the FAD environment (possibly related with FAD release from the MCAD protein), while monitoring the intrinsic tryptophan fluorescence ($dfDSF_{ITF}$; black lines in Fig. S7A–C) allowed to follow the denaturation of the protein. Nevertheless, $dfDSF_{FAD}$ was only possible for flavin-loaded variants, since the flavin-depleted p.D143V and p.Y372N variants exhibited no significant FAD-derived fluorescence (Fig. S7C). The calculated $T_{50(FAD)}$ values (Table 3) indicate a lower stability of the FAD cofactor in the p.Y48C, p.Y133C, p.A140T and p.K304E variants as compared to WT MCAD. The difference between fitted T_{m1} and T_{m2} values from $dfDSF_{ITF}$ was variant-dependent, ranging from 2.8 to 10.8 °C. For simplicity of analysis, the two values were weighted according to the relative contributions of each transition and a T_{mAVE} was calculated. As observed in Table 3, the variants p.Y48C, p.Y133C, p.A140T, p.D143V, p.K304E and p.Y372N exhibit lower thermal denaturation resistance than WT MCAD ($T_{mAVE(WT)}$ - $T_{mAVE(variant)} > -2.0$ °C), whereas the p.G377V variant exhibits increased thermal stability.

In addition, $dfDSF_{FAD}$ and $dsDSF_{ITF}$ data also offered the possibility to compare the changes in FAD environment and protein denaturation events. Notably, the onset of FAD-derived fluorescence increase preceded global protein denaturation in all variants. However, by analyzing the $T_{50(FAD)}$, FAD appears to dissociate concurrently with protein denaturation, apparently maintaining its association with the protein until the later events of protein unfolding (T_{mAVE}).

The kinetics of thermal denaturation was studied by ITDF experiments at 42 °C, in the absence or presence of additional FAD (Fig. S8). At this high fever-mimicking temperature, and with no supplementation of FAD, all the variants exhibited faster rates of denaturation (*k*) than the WT MCAD ($\Delta k > 50$ F·min^{-1}) whereas the p.G377V exhibited a lower denaturation rate (Δk of −88 F·min^{-1}) as shown in Table 4 and Fig. 4.

In the presence of 80 μM of FAD, all the MCAD proteins (WT and variants) exhibited considerably lower denaturation rates than in the absence of FAD (Table 4; Fig. S8B). However, when the Δk values obtained in the absence and presence of FAD were compared (Fig. 4), for the Y133C and p.D143V variants no statistical significance was observed. Nevertheless, in the presence of the cofactor all the variants still unfolded with slightly higher rates than WT, with the p.G377V remaining the single variant in which the kinetics of thermal unfolding was found to be similar to WT (Table 4; Figs. 4 and S8B).

In addition to the structural thermal stability, assays were performed to analyse the functional thermal stability. To this end, thermal inactivation profiles were obtained by incubating the MCAD WT and variants at various temperatures and then measuring the activity at 25 °C. The midpoint of thermal inactivation, $T_{1/2}$, was calculated taking the activity

Table 2
Kinetic parameters of recombinant wild-type (WT) and Group I and Group II variant medium chain acyl-CoA dehydrogenase (MCAD) tetramers towards octanoyl-CoA (C8-CoA).

		V_{max} (μmol DCPIP·min^{-1}·mg^{-1})	K_M (μM)	Catalytic efficiency[b] (μM^{-1}·min^{-1})
WT		1.57 ± 0.10	13.2 ± 1.9	9.7 ± 1.2
Group I	p.Y48C	0.62 ± 0.05***	5.4 ± 2.9*	10.6 ± 3.9
	p.Y133C	0.21 ± 0.04***	5.3 ± 3.4*	4.2 ± 2.3*
	p.A140T	0.66 ± 0.07***	6.3 ± 2.1*	8.8 ± 1.8
	p.D143V	_[c]	_[c]	_[c]
	p.Y372N[a]	_[c]	_[c]	_[c]
	p.R55G	1.83 ± 0.09	26.2 ± 2.4***	5.6 ± 0.3**
	p.G224R	0.66 ± 0.06***	7.6 ± 0.8*	7.0 ± 0.7*
Group II	p.V264I	2.04 ± 0.05**	25.1 ± 2.4**	6.5 ± 0.5*
	p.K304E	1.25 ± 0.06*	15.3 ± 2.4	6.6 ± 0.7*
	p.G377V	_[c]	_[c]	_[c]

Notes: (Group I) low FAD content; (Group II) FAD content similar to WT. Values represent $\overline{X} \pm S.D.$ of at least three independent expression and purification assays each performed in triplicate. *P* values (*<0.05, **<0.01, ***<0.005 and ****$P < 0.0001$) were calculated comparing recombinant MCAD variant values with the recombinant WT MCAD. All assays were performed using the PMS/DCPIP assay.

[a] p.Y372N dimers.

[b] Catalytic efficiency was calculated using the molecular mass of the tetramer.

[c] For variants with very low enzyme activities it was not possible to accurately determine the kinetic parameters.

obtained at 25 °C as 100 % (Fig. S9). As shown in Table 4, all variants except the p.R55G and p.K304E presented $T_{1/2}$ values statistically significantly different from the WT (56.8 ± 1.0 °C). The remaining variants showed lower $T_{1/2}$ with decreases ranging from −3.8 °C (p.G224R) to −8.3 °C (p.A140T).

Limited proteolysis by trypsin was performed to probe the conformational stability of MCAD variants. Under the tested conditions, WT MCAD appeared remarkably resistant to proteolysis by trypsin, with only ~30 % of the full-length protein band disappearing after 2 h (Table 4). Therefore, the percentage of full-length protein remaining intact at the plateau ($FL_{Plateau}$) was used to assess the resistance of MCADs for proteolysis. Whereas the p.Y133C, p.G224R, and p.V264I variants exhibited WT-like behaviour, the p.R55G, p.K304E and p.G377V variants appeared more resistant to proteolysis. On the opposite, the p.Y48C, p.A140T, p.D143V and p.Y372N variants were more sensitive to trypsin, particularly the latter two variants, which became totally degraded (Table 4; Fig. S10). Notably, FAD addition led to an increased resistance to proteolytic digestion, reflected in the 80–94 % of full-length protein retained after 120 min for recombinant MCAD WT as well as for the p.A140T, p.V264I and p.G377V variants. For the p.R55G, p.Y133C, p.G224R, and p.K304E variants, the FAD-protection was so effective that it precluded detecting any significant proteolysis up to 120 min. Only the flavin-depleted p.D143V and p.Y372N variants seemed unresponsive and displayed similar proteolytic profiles in the absence or presence of FAD.

4. Discussion

Over the last 20 years, the inclusion of the diagnosis of MCADD in newborn screening programmes in several countries led to a considerable improvement in the prognosis of the MCADD patients by allowing the introduction of early dietary and behavioural strategies to control the disease as well as to closely monitor the metabolic status of the patients which altogether greatly reduced the morbidity and mortality associated with this disease. However, whenever a metabolic challenge triggers decompensation, diagnosed patients are still at risk for clinical manifestations which may present a wide spectrum of severity, even for those patients with the same genotype. As for any other monogenic disorders, in MCADD the pathogenic phenotype will depend not only on the patient genotype but also on additional extrinsic and/or intrinsic factors yet to be fully understood. In this study, we aimed to explore the role of FAD, acyl-CoA MCAD substrate chain lengths and ETF interactions on the structure and activity of disease-associated MCAD variants. For this purpose, we studied 12 amino acid substitutions in the MCAD sequence. These substitutions are scattered along the three protein domains (Fig. S11), namely the αND (p.Y48C, p.R55G and p.A88P), βD (p.Y133C, p.A140T, p.D143V and p.G224R) and αCD (p.L238F, p.V264I, p.K304E, p.Y372N and p.G377V). From the studied proteins, only the p.A88P and p.L238F variants were recovered mainly in the insoluble fraction of the cell lysate, precluding their characterization, and suggesting that these amino acid changes lead to

Table 3
Thermal denaturation parameters of recombinant wild-type (WT) and Group I and Group II variant medium chain acyl-CoA dehydrogenase (MCAD) tetramers obtained by Far-UV circular dichroism (Far-UV CD) and dye-free differential scanning fluorimetry (dfDSF) monitoring the flavin fluorescence ($dfDS_{FAD}$) and intrinsic tryptophan fluorescence ($dfDSF_{ITF}$).

		Far-UV CD	$dfDSF_{ITF}$				$dfDSF_{FAD}$
		T_m (°C)	T_{m1} (°C)	T_{m2} (°C)	Frac	T_{mAVE} (°C)[a]	$T_{50(FAD)}$ (°C)
WT		54.0 ± 1.5	52.5 ± 0.1	59.2 ± 0.2	0.66 ± 0.02	54.7 ± 0.1	57.5 ± 0.1
Group I	p.Y48C	**49.0 ± 0.1**	47.7 ± 0.2	51.7 ± 0.2	0.58 ± 0.09	**49.0 ± 0.1**	**46.3 ± 0.3**
	p.Y133C	**51.6 ± 0.1**	49.7 ± 1.9	53.5 ± 0.3	0.37 ± 0.24	**52.4 ± 0.1**	**53.4 ± 0.3**
	p.A140T	**50.1 ± 0.1**	48.9 ± 0.1	52.1 ± 0.1	0.46 ± 0.01	**50.6 ± 0.1**	**50.9 ± 0.3**
	p.D143V	**49.1 ± 0.1**	48.3 ± 0.1	51.1 ± 0.1	0.58 ± 0.01	**49.5 ± 0.1**	n/a
	p.Y372N[b]	**46.4 ± 0.2**	45.7 ± 0.1	48.7 ± 0.1	0.54 ± 0.01	**47.0 ± 0.1**	n/a
	p.R55G	53.2 ± 0.2	52.7 ± 0.2	59.2 ± 0.1	0.49 ± 0.01	56.0 ± 0.1	59.1 ± 0.1
	p.G224R	52.4 ± 0.5	51.7 ± 0.1	58.6 ± 0.1	0.57 ± 0.01	54.6 ± 0.1	57.9 ± 0.3
Group II	p.V264I	**50.8 ± 0.1**	49.1 ± 0.3	56.8 ± 0.1	0.46 ± 0.01	53.2 ± 0.2	56.3 ± 0.1
	p.K304E	**49.0 ± 0.4**	45.7 ± 0.3	54.6 ± 0.2	0.43 ± 0.01	**50.8 ± 0.3**	**53.8 ± 0.3**
	p.G377V	55.6 ± 0.1	51.8 ± 1.8	62.6 ± 0.1	0.35 ± 0.01	58.8 ± 0.3	63.2 ± 0.2

Notes: (Group I) low FAD content; (Group II) FAD content similar to WT; Bold, T_m and $T_{50(FAD)}$ values considered significant when $\Delta T_m > -2.0$ °C. (n/a) not assessed.

[a] $T_{mAVE} = T_{m1}\cdot Frac + T_{m2}\cdot(1 - Frac)$.

[b] p.Y372N dimers.

Table 4
Kinetics of thermal denaturation (k) at 42 °C, thermal midpoint of enzymatic inactivation ($T_{1/2}$) and proteolytic stability ($FL_{Plateau}$) of recombinant wild-type (WT) and Group I and Group II variant medium chain acyl-CoA dehydrogenase (MCAD) tetramers in the absence (−FAD) or presence of 80 μM FAD (+FAD).

		k[b] (F·min^{-1})		$T_{1/2}$[c] (°C)	$FL_{Plateau}$[d] (%)	
		−FAD	+FAD		−FAD	+FAD
WT		508 ± 4.6	83 ± 2.3	56.8 ± 1.0	66.8 ± 2.9	94.2 ± 0.5
Group I	p.Y48C	863 ± 11.4	175 ± 4.3	49.1 ± 0.7***	47.8 ± 4.1**	79.7 ± 1.4***
	p.Y133C	564 ± 28.6	116 ± 6.4	51.8 ± 0.7 *	56.2 ± 3.0*	94.0 ± 0.5
	p.A140T	831 ± 27.0	121 ± 4.8	48.5 ± 0.6***	46.6 ± 5.2**	90.6 ± 0.6**
	p.D143V	688 ± 17.3	280 ± 10.0	n/a	n.d.	n.d.
	p.Y372N[a]	2084 ± 204	1053 ± 135	n/a	n.d.	n.d.
Group II	p.R55G	640 ± 15.9	97 ± 4.0	57.6 ± 1.1	87.8 ± 0.8**	97.0 ± 0.4**
	p.G224R	661 ± 6.6	132 ± 3.0	53.1 ± 0.7 **	74.6 ± 1.2*	95.8 ± 0.5*
	p.V264I	1818 ± 19.5	108 ± 8.4	49.7 ± 0.7***	69.1 ± 1.5	83.3 ± 0.8***
	p.K304E	736 ± 23.4	109 ± 8.8	55.4 ± 0.5	80.4 ± 1.9**	95.0 ± 0.7
	p.G377V	420 ± 14.2	93 ± 7.0	n/a	77.1 ± 1.3**	93.8 ± 2.3

Notes: (Group I) low FAD content; (Group II) FAD content similar to WT; (n/a) Not assessed; (n.d.) Not detected.

[a] p.Y372N dimers.

[b] The kinetics of thermostability was determined at 42 °C using isothermal denaturation fluorimetry (ITDF).

[c] The enzymatic assays were performed using the PMS/DCPIP assay and the C8-CoA substrate at 33 μM. Values represent $\overline{X} \pm S.D.$ of at least three independent expression and purification assays each performed in triplicate; P (*<0.05, **<0.01, ***<0.005 and ****P < 0.0001) was calculated comparing MCAD variant values with the WT.

[d] P values (*<0.05, **<0.005 and ***<0.0001) were calculated by comparing the variant MCADs with the WT; a P < 0.005 (not indicated in the table) was calculated for all the recombinant proteins (WT and variants) when data was obtained in the presence or absence of FAD (−FAD).

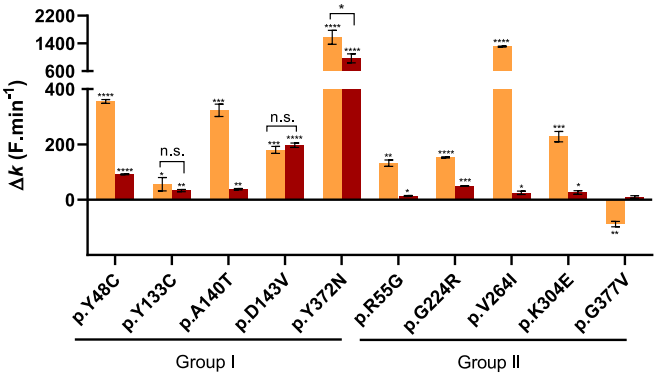

Fig. 4. Kinetics of thermal denaturation of wild-type (WT) and variant forms of medium chain acyl-CoA dehydrogenase (MCAD) at 42 °C determined by isothermal denaturation fluorimetry (ITDF). The denaturation rate (k) of MCADs were determined in the absence (■) or presence of 80 μM of FAD (■) and the values obtained for the variants were compared to the WT to obtain Δk. The data represents the mean ± SD of three replicates. P values (*<0.05, **<0.005, ***<0.0001 and ****<0.00001) were calculated comparing MCAD variant values with the WT. Regarding the comparative statistical analysis of the data obtained in the presence and absence of FAD only values not statistically different (n.s.) or with P < 0.05 are shown.

protein structures highly prone to aggregation. The Ala88 residue is localized at the αND (end of the α-helix D) and among the studied variants the p. A88P presented the lowest value of predicted pseudo ΔΔG (−4.49; Table S1) indicating a highly unstable protein. The bulkier side chain of a Pro in residue 88 increases the steric clashes (n = 5) with the surrounding residues and the substitution of Ala by a rigid amino acid as Pro may also disrupt α-helix D. Regarding the p.L238F variant, the affected residue is localized at αCD (within the βD connecting loop) buried in a small hydrophobic cavity. Replacing a methyl (Leu) by a benzyl (Phe) side chain substantially increases the number of steric clashes (n = 17) with the surrounding residues, therefore presenting a high propensity to disturb this protein region. The remaining ten MCAD variants were found in the soluble fraction of the cell lysate and although obtained in different yields it was possible to isolate the biological relevant tetramers except for the p.Y372N variant that was mainly recovered as dimers, which were the oligomeric species studied in this work.

The FAD cofactor is non-covalently bound to the protein and has an important role not only for the enzymatic reaction to occur but also on MCAD assembly and stability [12,51,60], as it has been demonstrated to be necessary for proper folding inside the mitochondria [8,9]. By studying non-conservative amino acid substitutions in FAD supplemented and non-supplemented culture media and buffers, Saijo and coworkers [10] showed that some variants can bind the cofactor during protein synthesis but its FAD-binding capacity is weak, thus prone to cofactor loss. Therefore, in this work, we focused on the study of the potential correlation of this protein component with the function and structure of disease-associated MCAD variants and by this mean to investigate their pathogenic relevance. In previous work from our group [43], expression and purification of MCAD (WT and p.K304E) has been performed in the absence of FAD supplementation. However, anticipating that in MCAD variants the FAD binding could be impaired, and to avoid loss of the cofactor under the stress conditions imposed during sonication, cell lysis was always performed in buffer supplemented with FAD as described in the literature [51]. However, no additional FAD was added during protein purification and storage as described by some authors [5]. This lysis/purification strategy may explain the slight differences observed in enzyme activity and thermostability when reported data are compared.

Among the three structural domains of MCAD the βD has an important role in FAD binding. Therefore, not surprisingly, three out of the four variants studied in this work belonging to the βD domain (p. Y133C, p.A140T and p.D143V) presented a FAD content/subunit 65 % lower than WT (Group I: p.Y48C, p.Y133C, p.A140T, p.D143V and p. Y372N). Tyr133 is in close proximity to the flavin isoalloxazine ring [11] and Ala140 and Asp143 belong to the Glu137-Asp143 loop which is essential for correctly positioning the ribityl moiety of FAD [7]. Amino acid changes in these residues will likely contribute to changes in the architecture of the cofactor binding pocket. Nevertheless, FAD also establishes contacts with the αCD, in particular with the α-helix K from its own subunit that can justify the low content of FAD/subunit observed in the case of the p.Y372N dimers (Group I) as the Tyr372 residue localizes at α-helix K and its substitution by Asn may interfere with FAD positioning. Likewise, FAD interacts with residues from the αCD of the neighbouring subunit, in particular the adenosine moiety that is surrounded by the loop between the α-helices G and H. The Lys304 residue is localized on α-helix H and our previous data from molecular dynamic simulations indicate a change in the architecture of the FAD binding pocket as well as on the FAD binding affinity for one of the dimers while the other remained unaffected [43]. These observations may explain why the FAD content/subunit of the p.K304E variant was ≈75 % of the WT recombinant MCAD. Regarding the p.Y48C variant, that also presents a low FAD content, it localizes at the αND, for which no direct involvement with FAD pocket/binding has been established so far.

In order to identify among the studied parameters which were most influenced by the FAD content, correlation tests were performed against

FAD affinity, thermostability, proteolytic stability and thermal inactivation of the studied MCAD proteins (Fig. 5). An association was found between FAD content/subunit and binding affinity for the cofactor (lower FAD content → higher k_B; Fig. 5A), $T_{50(FAD)}$ (monitoring FAD displacement; Fig. 5B), thermal stability of the protein structure (Fig. 5C and D: T_m and T_{mAVE}), resistance to proteolysis (Fig. 5E; $FL_{plateau}$) and thermal inactivation (Fig. 5F: $T_{1/2}$). These data indicate a strong dependence of the enzyme stability on the structural presence of the FAD cofactor. This is particularly evident from the obtained proteolytic stability data, as the variants presenting the lowest level of FAD (p.D143V and p.Y372N) were the proteins more prone to limited proteolysis. The susceptibility of proteins to controlled proteases digestion reveals the exposure of specific protein regions which are targets for proteolysis [61,62].

Taken together, it is very likely that the absence of FAD will contribute to the generation of proteins with less rigid/more flexible conformations, exposing the target sequences to trypsin hydrolysis. In contrast, the FAD content/subunit did not correlate with the percentage of tetrameric forms, suggesting that even within the assembled subunits of the tetramer it is possible that the FAD binding sites are not fully occupied. Nevertheless, the only MCAD variants with disturbed oligomeric profiles (p.Y48C, p.D143V and p.Y372N), which presented high levels of aggregates (p.D143V) and dimers (p.Y48C and p.Y372N), also showed a low FAD content/subunit namely 0.56 (p.Y48C), ≈0 (p.D143V) and 0.23 (p.Y372N). The recovery of p.D143V tetramers with almost null FAD content indicates structural viability of tetramers devoid of cofactor, although presenting low stability and lacking enzymatic activity. Similarly, no correlation was observed when the FAD content was analysed against the denaturation rate at 42 °C (k), indicating that FAD did not directly contribute to faster kinetics of denaturation. Remarkably, in those *in vitro* assays where FAD supplementation was tested (limited proteolysis and kinetics of thermal denaturation) it was evident that most of the studied variants responded to the cofactor increasing the resistance to proteolysis (except the p.D143V and p.Y372N variants) and to thermal unfolding (except the p.Y133C, p.D143V and p.Y372N variants to some extent).

At the functional level, and as expected Group I proteins (lower FAD content: p.Y48C, p.Y133C, p.A140T, p.D143V and p.Y372N dimers) also

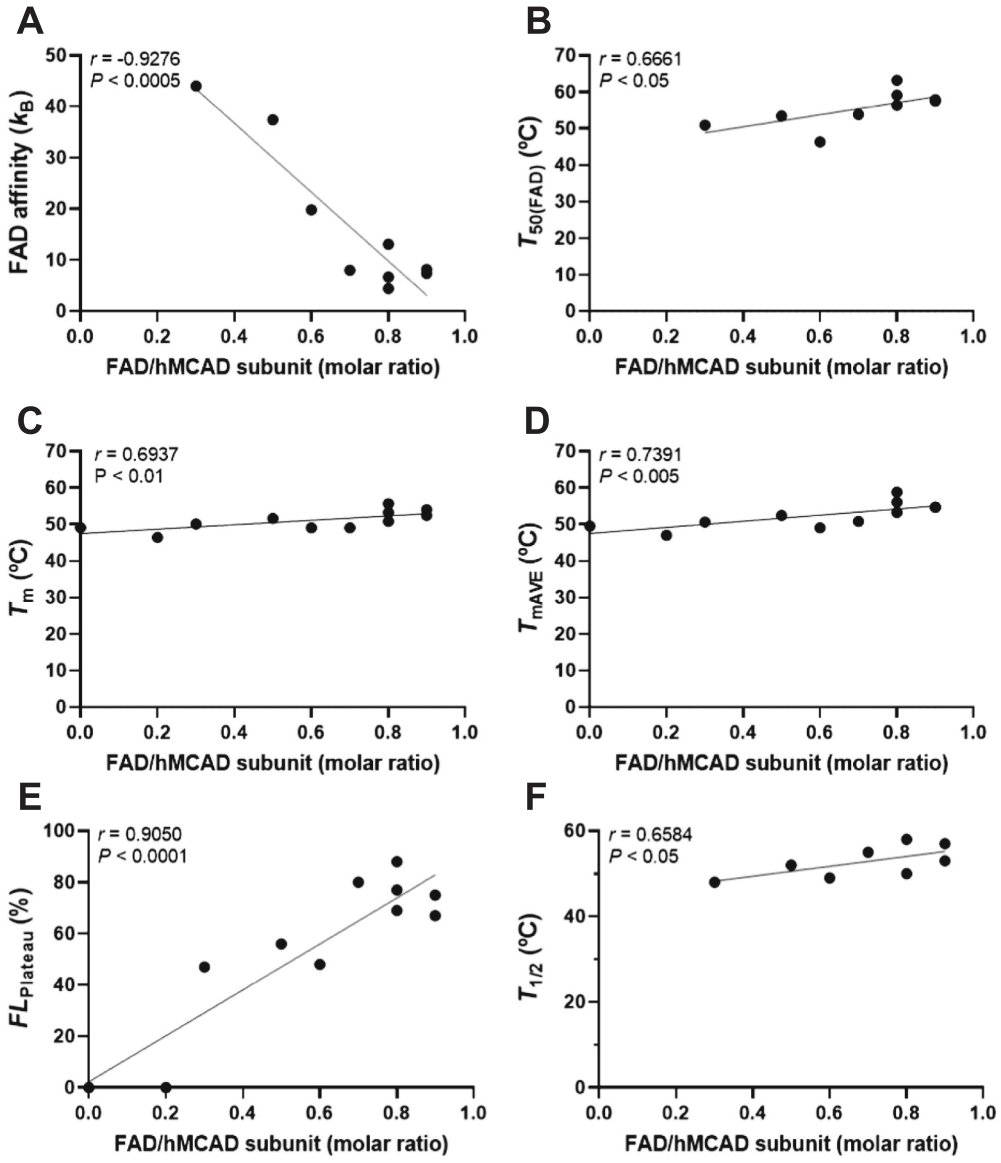

Fig. 5. Association of FAD content/subunit with FAD affinity (A), FAD displacement (B), thermostability (C and D), proteolytic stability (E) and thermal inactivation (F) of recombinant medium chain acyl-CoA dehydrogenase (MCAD) wild-type (WT) and variants. The correlation between data was determined with the Pearson Correlation assay using GraphPad Prism to obtain the correlation coefficient (r) and P.

presented lower residual enzymatic activity towards the tested acyl-CoAs (<50 % of recombinant WT MCAD activity), and for those variants for which kinetic parameters were obtained (p.Y48C, p.Y133C and p.A140T) lower V_{max} values were also observed. However, the FAD content was not the single factor contributing to a relative enzyme activity lower than the WT. Indeed, the p.G224R and p.G377V and variants (belonging to Group II: FAD occupancy approaching the WT) presented respectively ≈40 % of WT and almost null activity. These data indicate that, as expected, other factors, besides the presence of the cofactor, are involved in the enzymatic reaction. The Gly377 residue is localized on the αCD in an adjacent position to the catalytic residue Glu376. It is expected that the substitution of Gly377 by Val, an amino acid with a longer side chain, will impact the conformation and local environment of this region necessary for the chemical reaction to occur, thus contributing to the low level of enzyme activity. The p.R55G and p.V264I variants, although presenting residual enzyme activities >80 % for all the tested substrates, showed a low affinity for the C8-CoA substrate thus affecting the enzyme's catalytic efficiency. Val264 is localized at the αCD, within the α-helix G, a long secondary structure with its N-terminus (Ala243) localized at the protein surface (delineating the entrance of the catalytic pocket) and the C-terminus (Leu279) deeply buried and lining the acyl moiety of the substrate. The substitution of Val by Ile in position 264 may disturb the local helical packing arrangement with a direct influence on the pocket architecture, thus rendering a protein with low affinity for the substrate. The Arg55 residue is positioned at α-helix C (αND) in a solvent-exposed region, its side chain being within electrostatic interaction distance with the side chain of Glu34 from the neighbouring helix. This interaction is lost by replacement of Arg55 with Gly, likely causing a local disturbance in terms of packing of neighbouring helices that propagate to the active site. Similar long-distance effects of pathogenic substitutions propagating flexibility/instability to the active site and thereby affecting substrate affinity have been observed in pyruvate dehydrogenase complex E1 component [63].

Regarding MCAD activity towards acyl-CoA substrates with different chain-lengths, as the acyl group of the substrate is buried into the catalytic pocket, it is expected that substrates with smaller chain-lengths can be accommodated more easily than longer acyl chains with the concomitant impact on enzyme activity (C6 > C8 > C10 > C12) [4,5]. However, four (p.Y133C p.R55G, p.G224R and p.K304E) out of the ten studied variants did not present the expected chain-length dependence. The higher activity obtained for the p.Y133C variant in the presence of C12-CoA indicates that the structural changes that lead to low incorporation of FAD leave the catalytic pocket more prone to accommodate acyl-CoA substrates with higher chain-lengths. The p.R55G variant showed lower residual activity in the presence of C8-CoA, which can be associated with the lower affinity determined for this substrate, while the p.G224R and p.K304E variants presented similar residual activities towards the C6- and C8-CoA substrates, indicating that for these enzymes no discrimination for acyl-CoAs of shorter chain-lengths occurs. Noteworthy, five out of the seven variants for which catalytic parameters were possible to be evaluated, showed catalytic efficiencies (towards C8-CoA) lower than for the WT due to a disturbed V_{max} and/or K_M. These data, not only support the pathogenic effect of the studied *ACADM* gene mutations, but also highlights the need for a careful evaluation of the enzymatic assay conditions usually performed in patient cells (such as cultured fibroblast and lymphocytes) for the diagnosis of MCADD. In fact, these assays are usually performed at V_{max} conditions with saturating concentrations of substrate and from our data each variant will present its optimal activity range. Therefore, enzymatic assays should be run at substrate concentration ranges near/bellow the enzyme K_M as already reported for other enzymes such as phenylalanine hydroxylase [64] and pyruvate dehydrogenase [63]. Of note, for the majority of the studied MCAD variants, the temperature has an impact on the enzyme's activity (shifting $T_{1/2}$ to lower values). In addition, the higher $\Delta k_{42^\circ C}$ observed also indicates that most of the variants are conformationally susceptible to temperature levels that occur in case of fever, which could be envisaged as a mechanism underlying the metabolic decompensation of MCADD patients in case of infections which frequently lead to coma and death if not early intervened.

Within a biological context, the correct folding of MCAD is reciprocally required for FAD incorporation/maintenance, for the architecture of the catalytic pocket and importantly it is also necessary for the establishment of MCAD/ETF interactions. In this work, we aimed to understand if the amino acid changes occurring in the disease-associated MCAD variants which we studied, could disrupt these interactions. To this end, using the C8-CoA substrate, enzymatic assays were performed in the presence of the ETF/DCPIP pair, and the obtained data were compared with those determined using the artificial pair PMS/DCPIP. Five variants (p.Y48C, p.A140, p.D143V p.V264I and p.G377V) out of the ten variants studied, did not impact MCAD/ETF interaction and/or electron transfer among the respective FAD, as no statistically significant differences on residual enzyme activities were found among the two assays. The amino acid changes introduced in the p.R55G, p.G224R and p.K304E MCAD variants led to lower catalytic activities in the ETF/DCPIP assay indicating an effect on the MCAD/ETF interaction and/or electron flux. In the case of the p.R55G variant, the involved residue is localized at α-helix C, which together with α-helix D, has been described to establish contacts with the recognition loop of ETF localized on the EFT-β (Arg191 to Lys200). It is expected that substitution of the positively charged Arg residue by a small, flexible and hydrophobic residue (Gly) will contribute to changes in the conformation of this region that can compromise MCAD/ETF interactions. For the p.G224R and p.K304E variants, the affected residues are localized far from the MCAD/ETF interacting region. However, it has been postulated that upon binding of the ETF-β to the αND of MCAD, the ETF-α, harbouring the FAD cofactor, will move towards the βD of the adjacent MCAD subunit approaching the two FAD molecules (14 Å rule) with the involvement of the Arg249 of ETF-α and of the Glu212 localized at β-strand 6 of MCAD [21]. In this case, the substitution of a small hydrophobic amino acid (Gly) in residue 224 of β-strand 7 by a larger and positively charged residue will disturb this region probably affecting the Glu212 (MCAD)/Arg249 (ETF-α) interaction and/or electron transfer between the two FAD molecules. Interestingly, for the p.Y133C and p.Y372N variants a higher residual activity was obtained when using the ETF/DCPIP assay suggesting that MCAD/ETF interaction or electron flux between the two FAD molecules may actually be enhanced as a consequence of these amino acid changes.

The high levels of dimeric forms presented by the p.Y48C and p.Y372N suggest that the tetramers of these variants are unstable structures that tend to dissociate or that MCAD subunits are unable to assemble as tetramers, an effect much more pronounced in the case of the later variant which was recovered mainly as dimers. As expected, the p.Y372N dimers presented defective FAD incorporation, low residual enzyme activity, and decreased proteolytic- and thermal-stability. Assembly of the tetramers is promoted by interactions between the α-helices G and H (αCD) of one dimer and the α-helices I and K (αCD) of the corresponding subunit of the neighbouring dimer [41]. As such localization of p.Y372N on α-helix K of the αCD may affect MCAD tetramerization. However, concerning the p.Y48C its localization within the αND, in the loop connecting α-helices A and B, and far from the protein secondary structures that are involved in the tetrameric assembly does not provide any direct suggestion on the effect of Tyr to Cys change on MCAD tetramerization.

According to previous studies on recombinant MCAD variants, it has been shown that amino acid changes located in the α-helices of the αCD, which is involved in the stabilization of the tetramer, have a high propensity to disrupt the assembly process leading to protein aggregation. Variant proteins with substitutions in amino acids in the central βD and in the loops interconnecting this domain and the αCD are particularly unstable and prone to conformational changes [30–32]. Moreover, variant proteins with amino acid substitutions localized in the αND have shown moderate effects on tetramer assembly and thermal stability, as

well as on catalytic activity [32,65]. However, in our study, we found that amino acid substitutions in the αND can also contribute to structural instability (p.A88P), changes in protein assembly, decreased FAD content (p.Y48C) and lower affinity for the C8-CoA substrate (p.R55G). These data suggest that intricate networks of non-covalent interactions occur accounting to MCAD conformation and assembly as well as substrate affinity and cofactor binding. Moreover, even amino acid substitutions in residues far from the substrate and FAD binding pockets or from the helical bundle directly involved in the tetramer assembly, could have an impact on protein function and structure. These hypotheses require further investigation.

Amino acid substitutions in the αND can similarly strongly affect enzyme activity and/or electron transfer when enzyme activity is measured using the ETF/DCPIP assay (p.R55G). Therefore, it is expected that for some of the variant MCAD proteins their enzymatic activity in a biological context will be lower when compared with *in vitro* studies, especially if artificial electron pairs have been used, thus contributing to the observed inconsistencies when genotype/phenotype correlations were investigated. In our study the performed thermal denaturation assays suggest that most of the characterized variants are structurally unstable *in vitro* but no direct data on protein misfolding was obtained to confirm this. In the mitochondrial environment protein misfolding is an important player as it can lead to aggregation and premature degradation.

According to our data, the majority of variant MCADs presented an impaired capacity to retain the cofactor within their structure, and some of them were structurally "responsive" to cofactor supplementation. Therefore, we may postulate that in the mitochondrial environment the levels and activity of those variants will also be dependent on the availability of FAD, as already observed for other ACADMs [51]. In this perspective, and as the precursor of FAD, riboflavin (vitamin B2) status will have an impact not only on the activity of the MCAD variants but also on their structural stability. Before being used for the intracellular synthesis of FAD, riboflavin must be absorbed and transported through a complex system of transporters and enzymes. Riboflavin levels are thus strongly dependent on several factors such as genetics, inflammation and infections, exercise, diet and malnutrition, aging and pregnancy [66]. Due to these factors several studies indicate that insufficient riboflavin status is more frequent than expected, even in populations where riboflavin-rich diets are consumed [66]. Concerning MCADD patients, it would be important to monitor their riboflavin status particularly during episodes of decompensation. In addition, the effect of riboflavin supplementation on the clinical status of MCADD patients should also be addressed as only two studies have been carried out to date within a restrict number of patients and with no follow-up of the clinical outcome [67,68].

Overall, for the recombinant MCAD variants analysed in this study, the molecular basis of pathogenicity can be assumed. Even for those proteins where the amino acid substitutions did not greatly impact the structure of the protein, an effect on enzyme activity was observed such as the low affinity for the C8-CoA substrate (p.V264I) or a defective interaction with ETF (p.R55G) either at a structural or at a functional level that can impact the patient phenotype.

CRediT authorship contribution statement

Catarina A. Madeira: Investigation, Formal analysis, Writing – original draft. **Carolina Anselmo:** Investigation. **João M. Costa:** Investigation. **Cátia A. Bonito:** Resources, Writing – review & editing, Funding acquisition. **Ricardo J. Ferreira:** Resources, Writing – review & editing, Funding acquisition. **Daniel J.V.A. Santos:** Resources, Writing – review & editing. **Ronald Wanders:** Resources, Writing – review & editing. **João B. Vicente:** Methodology, Formal analysis, Writing – review & editing. **Fátima V. Ventura:** Conceptualization, Writing – review & editing, Supervision, Funding acquisition. **Paula Leandro:** Conceptualization, Formal analysis, Writing – original draft, Supervision.

Declaration of competing interest

The authors declare that they have no known competing financial interests or personal relationships that could have appeared to influence the work reported in this paper.

Data availability

Data will be made available on request.

Acknowledgments

This work was supported by FEDER and Fundação para a Ciência e a Tecnologia, I. P. through iMed.ULisboa (Projects UIDB/04138/2020 and UIDP/04138/2020), iNOVA4Health (UIDB/04462/2020, UIDP/04462/2020) and LS4FUTURE Associated Laboratory (LA/P/0087/2020) and research project PTDC/BIA-BQM/29570/2017.

The authors would like to thank Andreia Luz, Joana Nunes, Neža Palir, Filipa Louro, Francisca Vargas, Joana Camilo and João Leandro who contributed to the exploratory research that culminated in the work herein presented.

Appendix A. Supplementary data

Supplementary data to this article can be found online at https://doi.org/10.1016/j.bbadis.2023.166766.

References

[1] Y.Q. Shen, B.F. Lang, G. Burger, Diversity and dispersal of a ubiquitous protein family: acyl-CoA dehydrogenases, Nucleic Acids Res. 37 (2009) 5619–5631, https://doi.org/10.1093/nar/gkp566.

[2] S. Ghisla, C. Thorpe, Acyl-CoA dehydrogenases. A mechanistic overview, Eur. J. Biochem. 271 (2004) 494–508, https://doi.org/10.1046/j.1432-1033.2003.03946.x.

[3] M. He, Z. Pei, A.W. Mohsen, P. Watkins, G. Murdoch, P.P. Van Veldhoven, R. Ensenauer, J. Vockley, Identification and characterization of new long chain acyl-CoA dehydrogenases, Mol. Genet. Metab. 102 (2011) 418–429, https://doi.org/10.1016/j.ymgme.2010.12.005.

[4] A. Nandy, V. Kieweg, F.G. Krautle, P. Vock, B. Kuchler, P. Bross, J.J. Kim, I. Rasched, S. Ghisla, Medium-long-chain chimeric human Acyl-CoA dehydrogenase: medium-chain enzyme with the active center base arrangement of long-chain Acyl-CoA dehydrogenase, Biochemistry 35 (1996) 12402–12411, https://doi.org/10.1021/bi960785e.

[5] V. Kieweg, F.G. Krautle, A. Nandy, S. Engst, P. Vock, A.G. Abdel-Ghany, P. Bross, N. Gregersen, I. Rasched, A. Strauss, S. Ghisla, Biochemical characterization of purified, human recombinant Lys304–>Glu medium-chain acyl-CoA dehydrogenase containing the common disease-causing mutation and comparison with the normal enzyme, Eur. J. Biochem. 246 (1997) 548–556, https://doi.org/10.1111/j.1432-1033.1997.00548.x.

[6] B.S. Andresen, T.G. Jensen, P. Bross, I. Knudsen, V. Winter, S. Kolvraa, L. Bolund, J. H. Ding, Y.T. Chen, J.L. Van Hove, et al., Disease-causing mutations in exon 11 of the medium-chain acyl-CoA dehydrogenase gene, Am. J. Hum. Genet. 54 (1994) 975–988.

[7] J.J. Kim, M. Wang, R. Paschke, Crystal structures of medium-chain acyl-CoA dehydrogenase from pig liver mitochondria with and without substrate, Proc. Natl. Acad. Sci. U. S. A. 90 (1993) 7523–7527, https://doi.org/10.1073/pnas.90.16.7523.

[8] T. Saijo, W.J. Welch, K. Tanaka, Intramitochondrial folding and assembly of medium-chain acyl-CoA dehydrogenase (MCAD). Demonstration of impaired transfer of K304E-variant MCAD from its complex with hsp60 to the native tetramer, J. Biol. Chem. 269 (1994) 4401–4408.

[9] T. Saijo, K. Tanaka, Isoalloxazine ring of FAD is required for the formation of the core in the Hsp60-assisted folding of medium chain acyl-CoA dehydrogenase subunit into the assembly competent conformation in mitochondria, J. Biol. Chem. 270 (1995) 1899–1907, https://doi.org/10.1074/jbc.270.4.1899.

[10] T. Saijo, J.J. Kim, Y. Kuroda, K. Tanaka, The roles of threonine-136 and glutamate-137 of human medium chain acyl-CoA dehydrogenase in FAD binding and peptide folding using site-directed mutagenesis: creation of an FAD-dependent mutant, T136D, Arch. Biochem. Biophys. 358 (1998) 49–57, https://doi.org/10.1006/abbi.1998.0844.

[11] A. Satoh, Y. Nakajima, I. Miyahara, K. Hirotsu, T. Tanaka, Y. Nishina, K. Shiga, H. Tamaoki, C. Setoyama, R. Miura, Structure of the transition state analog of medium-chain acyl-CoA dehydrogenase. Crystallographic and molecular orbital studies on the charge-transfer complex of medium-chain acyl-CoA dehydrogenase

with 3-thiaoctanoyl-CoA, J. Biochem. 134 (2003) 297–304, https://doi.org/10.1093/jb/mvg143.
[12] J.J. Kim, R. Miura, Acyl-CoA dehydrogenases and acyl-CoA oxidases. Structural basis for mechanistic similarities and differences, Eur. J. Biochem. 271 (2004) 483–493, https://doi.org/10.1046/j.1432-1033.2003.03948.x.
[13] N. Gregersen, B.S. Andresen, C.B. Pedersen, R.K. Olsen, T.J. Corydon, P. Bross, Mitochondrial fatty acid oxidation defects–remaining challenges, J. Inherit. Metab. Dis. 31 (2008) 643–657, https://doi.org/10.1007/s10545-008-0990-y.
[14] I. Rudik, S. Ghisla, C. Thorpe, Protonic equilibria in the reductive half-reaction of the medium-chain acyl-CoA dehydrogenase, Biochemistry 37 (1998) 8437–8445, https://doi.org/10.1021/bi980388z.
[15] D.L. Roberts, F.E. Frerman, J.J. Kim, Three-dimensional structure of human electron transfer flavoprotein to 2.1-A resolution, Proc. Natl. Acad. Sci. U. S. A. 93 (1996) 14355–14360, https://doi.org/10.1073/pnas.93.25.14355.
[16] J. Zhang, F.E. Frerman, J.J. Kim, Structure of electron transfer flavoprotein-ubiquinone oxidoreductase and electron transfer to the mitochondrial ubiquinone pool, Proc. Natl. Acad. Sci. U. S. A. 103 (2006) 16212–16217, https://doi.org/10.1073/pnas.0604567103.
[17] S. Ghisla, Beta-oxidation of fatty acids. A century of discovery, Eur. J. Biochem. 271 (2004) 459–461, https://doi.org/10.1046/j.1432-1033.2003.03952.x.
[18] H.S. Toogood, A. van Thiel, J. Basran, M.J. Sutcliffe, N.S. Scrutton, D. Leys, Extensive domain motion and electron transfer in the human electron transferring flavoprotein.medium chain Acyl-CoA dehydrogenase complex, J. Biol. Chem. 279 (2004) 32904–32912, https://doi.org/10.1074/jbc.M404884200.
[19] C.C. Page, C.C. Moser, X. Chen, P.L. Dutton, Natural engineering principles of electron tunnelling in biological oxidation-reduction, Nature 402 (1999) 47–52, https://doi.org/10.1038/46972.
[20] C.C. Page, C.C. Moser, P.L. Dutton, Mechanism for electron transfer within and between proteins, Curr. Opin. Chem. Biol. 7 (2003) 551–556, https://doi.org/10.1016/j.cbpa.2003.08.005.
[21] H.S. Toogood, A. van Thiel, N.S. Scrutton, D. Leys, Stabilization of non-productive conformations underpins rapid electron transfer to electron-transferring flavoprotein, J. Biol. Chem. 280 (2005) 30361–30366, https://doi.org/10.1074/jbc.M505562200.
[22] R.J.A. Wanders, G. Visser, S. Ferdinandusse, F.M. Vaz, R.H. Houtkooper, Mitochondrial fatty acid oxidation disorders: laboratory diagnosis, pathogenesis, and the complicated route to treatment, J. Lipid Atheroscler. 9 (2020) 313–333, https://doi.org/10.12997/jla.2020.9.3.313.
[23] B. Wilcken, Fatty acid oxidation disorders: outcome and long-term prognosis, J. Inherit. Metab. Dis. 33 (2010) 501–506, https://doi.org/10.1007/s10545-009-9001-1.
[24] W.J. Rhead, Newborn screening for medium-chain acyl-CoA dehydrogenase deficiency: a global perspective, J. Inherit. Metab. Dis. 29 (2006) 370–377, https://doi.org/10.1007/s10545-006-0292-1.
[25] B.L. Therrell, C.D. Padilla, J.G. Loeber, I. Kneisser, A. Saadallah, G.J. Borrajo, J. Adams, Current status of newborn screening worldwide: 2015, Semin. Perinatol. 39 (2015) 171–187, https://doi.org/10.1053/j.semperi.2015.03.002.
[26] J. Purevsuren, Y. Hasegawa, S. Fukuda, H. Kobayashi, Y. Mushimoto, K. Yamada, T. Takahashi, T. Fukao, S. Yamaguchi, Clinical and molecular aspects of Japanese children with medium chain acyl-CoA dehydrogenase deficiency, Mol. Genet. Metab. 107 (2012) 237–240, https://doi.org/10.1016/j.ymgme.2012.06.010.
[27] F.V. Ventura, P. Leandro, A. Luz, I.A. Rivera, M.F. Silva, R. Ramos, H. Rocha, A. Lopes, H. Fonseca, A. Gaspar, L. Diogo, E. Martins, E. Leao-Teles, L. Vilarinho, I. Tavares de Almeida, Retrospective study of the medium-chain acyl-CoA dehydrogenase deficiency in Portugal, Clin. Genet. 85 (2014) 555–561, https://doi.org/10.1111/cge.12227.
[28] B.S. Andresen, A.M. Lund, D.M. Hougaard, E. Christensen, B. Gahrn, M. Christensen, P. Bross, A. Vested, H. Simonsen, K. Skogstrand, S. Olpin, N. J. Brandt, F. Skovby, B. Norgaard-Pedersen, N. Gregersen, MCAD deficiency in Denmark, Mol. Genet. Metab. 106 (2012) 175–188, https://doi.org/10.1016/j.ymgme.2012.03.018.
[29] G.F. Hoffmann, R. von Kries, D. Klose, M. Lindner, A. Schulze, A.C. Muntau, W. Roschinger, B. Liebl, E. Mayatepek, A.A. Roscher, Frequencies of inherited organic acidurias and disorders of mitochondrial fatty acid transport and oxidation in Germany, Eur. J. Pediatr. 163 (2004) 76–80, https://doi.org/10.1007/s00431-003-1246-3.
[30] J.M. Jank, E.M. Maier, D.D. Reibeta, M. Haslbeck, K.F. Kemter, M.S. Truger, C. P. Sommerhoff, S. Ferdinandusse, R.J. Wanders, S.W. Gersting, A.C. Muntau, The domain-specific and temperature-dependent protein misfolding phenotype of variant medium-chain acyl-CoA dehydrogenase, PLoS One 9 (2014), e93852, https://doi.org/10.1371/journal.pone.0093852.
[31] K.L. Koster, M. Sturm, D. Herebian, S.H. Smits, U. Spiekerkoetter, Functional studies of 18 heterologously expressed medium-chain acyl-CoA dehydrogenase (MCAD) variants, J. Inherit. Metab. Dis. 37 (2014) 917–928, https://doi.org/10.1007/s10545-014-9732-5.
[32] E.M. Maier, S.W. Gersting, K.F. Kemter, J.M. Jank, M. Reindl, D.D. Messing, M. S. Truger, C.P. Sommerhoff, A.C. Muntau, Protein misfolding is the molecular mechanism underlying MCADD identified in newborn screening, Hum. Mol. Genet. 18 (2009) 1612–1623, https://doi.org/10.1093/hmg/ddp079.
[33] P. Bross, B.S. Andresen, V. Winter, F. Krautle, T.G. Jensen, A. Nandy, S. Kolvraa, S. Ghisla, L. Bolund, N. Gregersen, Co-overexpression of bacterial GroESL chaperonins partly overcomes non-productive folding and tetramer assembly of E. coli-expressed human medium-chain acyl-CoA dehydrogenase (MCAD) carrying the prevalent disease-causing K304E mutation, Biochim. Biophys. Acta 1182 (1993) 264–274, https://doi.org/10.1016/0925-4439(93)90068-c.
[34] P. Bross, C. Jespersen, T.G. Jensen, B.S. Andresen, M.J. Kristensen, V. Winter, A. Nandy, F. Krautle, S. Ghisla, L. Bolundi, et al., Effects of two mutations detected in medium chain acyl-CoA dehydrogenase (MCAD)-deficient patients on folding, oligomer assembly, and stability of MCAD enzyme, J. Biol. Chem. 270 (1995) 10284–10290, https://doi.org/10.1074/jbc.270.17.10284.
[35] H. Piercy, C. Nutting, S. Yap, "It's just always eating": the experiences of young people growing up medium chain acyl-coA dehydrogenase deficiency, Glob. Qual. Nurs. Res. 8 (2021), 23333936211032203, https://doi.org/10.1177/23333936211032203.
[36] U.A. Schatz, R. Ensenauer, The clinical manifestation of MCAD deficiency: challenges towards adulthood in the screened population, J. Inherit. Metab. Dis. 33 (2010) 513–520, https://doi.org/10.1007/s10545-010-9115-5.
[37] A.C. Muntau, J. Leandro, M. Staudigl, F. Mayer, S.W. Gersting, Innovative strategies to treat protein misfolding in inborn errors of metabolism: pharmacological chaperones and proteostasis regulators, J. Inherit. Metab. Dis. 37 (2014) 505–523, https://doi.org/10.1007/s10545-014-9701-z.
[38] M.I. Mendes, D.E. Smith, J.B. Vicente, I. Tavares De Almeida, T. Ben-Omran, G. S. Salomons, I.A. Rivera, P. Leandro, H.J. Blom, Small aminothiol compounds improve the function of Arg to Cys variant proteins: effect on the human cystathionine beta-synthase p.R336C, Hum. Mol. Genet. 24 (2015) 7339–7348, https://doi.org/10.1093/hmg/ddv431.
[39] R.R. Lopes, C.S. Tome, R. Russo, R. Paterna, J. Leandro, N.R. Candeias, L.M. D. Goncalves, M. Teixeira, P.M.F. Sousa, R.C. Guedes, J.B. Vicente, P.M.P. Gois, P. Leandro, Modulation of human phenylalanine hydroxylase by 3-hydroxyquinolin-2(1H)-one derivatives, Biomolecules 11 (2021), https://doi.org/10.3390/biom11030462.
[40] M. Hole, J. Underhaug, H. Diez, M. Ying, A.K. Rohr, A. Jorge-Finnigan, N. Fernandez-Castillo, A. Garcia-Cazorla, K.K. Andersson, K. Teigen, A. Martinez, Discovery of compounds that protect tyrosine hydroxylase activity through different mechanisms, Biochim. Biophys. Acta 2015 (1854) 1078–1089, https://doi.org/10.1016/j.bbapap.2015.04.030.
[41] E.M. Maier, B. Liebl, W. Roschinger, U. Nennstiel-Ratzel, R. Fingerhut, B. Olgemoller, U. Busch, N. Krone, R. v Kries, A.A. Roscher, Population spectrum of ACADM genotypes correlated to biochemical phenotypes in newborn screening for medium-chain acyl-CoA dehydrogenase deficiency, Hum. Mutat. 25 (2005) 443–452, https://doi.org/10.1002/humu.20163.
[42] P. Bross, S. Engst, A.W. Strauss, D.P. Kelly, I. Rasched, S. Ghisla, Characterization of wild-type and an active site mutant of human medium chain acyl-CoA dehydrogenase after expression in Escherichia coli, J. Biol. Chem. 265 (1990) 7116–7119.
[43] C.A. Bonito, J. Nunes, J. Leandro, F. Louro, P. Leandro, F.V. Ventura, R.C. Guedes, Unveiling the pathogenic molecular mechanisms of the most common variant (p. K329E) in medium-chain acyl-CoA dehydrogenase deficiency by in vitro and in silico approaches, Biochemistry 55 (2016) 7086–7098, https://doi.org/10.1021/acs.biochem.6b00759.
[44] C.M. Touw, G.P. Smit, M. de Vries, J.B. de Klerk, A.M. Bosch, G. Visser, M. F. Mulder, M.E. Rubio-Gozalbo, B. Elvers, K.E. Niezen-Koning, R.J. Wanders, H. R. Waterham, D.J. Reijngoud, T.G. Derks, Risk stratification by residual enzyme activity after newborn screening for medium-chain acyl-CoA dehyrogenase deficiency: data from a cohort study, Orphanet J. Rare Dis. 7 (2012) 30, https://doi.org/10.1186/1750-1172-7-30.
[45] C.M. Touw, G.P. Smit, K.E. Niezen-Koning, C. Bosgraaf-de Boer, A. Gerding, D. J. Reijngoud, T.G. Derks, In vitro and in vivo consequences of variant medium-chain acyl-CoA dehydrogenase genotypes, Orphanet J. Rare Dis. 8 (2013) 43, https://doi.org/10.1186/1750-1172-8-43.
[46] E.A. Jager, M.M. Kuijpers, A.M. Bosch, M.F. Mulder, E.R. Gozalbo, G. Visser, M. de Vries, M. Williams, H.R. Waterham, F.J. van Spronsen, P. Schielen, T.G.J. Derks, A nationwide retrospective observational study of population newborn screening for medium-chain acyl-CoA dehydrogenase (MCAD) deficiency in the Netherlands, J. Inherit. Metab. Dis. 42 (2019) 890–897, https://doi.org/10.1002/jimd.12102.
[47] Y. Ikeda, K. Okamura-Ikeda, K. Tanaka, Spectroscopic analysis of the interaction of rat liver short-chain, medium-chain, and long-chain acyl coenzyme A dehydrogenases with acyl coenzyme A substrates, Biochemistry 24 (1985) 7192–7199, https://doi.org/10.1021/bi00346a027.
[48] P. Bross, P. Pedersen, V. Winter, M. Nyholm, B.N. Johansen, R.K. Olsen, M. J. Corydon, B.S. Andresen, H. Eiberg, S. Kolvraa, N. Gregersen, A polymorphic variant in the human electron transfer flavoprotein alpha-chain (alpha-T171) displays decreased thermal stability and is overrepresented in very-long-chain acyl-CoA dehydrogenase-deficient patients with mild childhood presentation, Mol. Genet. Metab. 67 (1999) 138–147, https://doi.org/10.1006/mgme.1999.2856.
[49] P. Augustin, M. Toplak, K. Fuchs, E.C. Gerstmann, R. Prassl, A. Winkler, P. Macheroux, Oxidation of the FAD cofactor to the 8-formyl-derivative in human electron-transferring flavoprotein, J. Biol. Chem. 293 (2018) 2829–2840, https://doi.org/10.1074/jbc.RA117.000846.
[50] F.H. Niesen, H. Berglund, M. Vedadi, The use of differential scanning fluorimetry to detect ligand interactions that promote protein stability, Nat. Protoc. 2 (2007) 2212–2221, https://doi.org/10.1038/nprot.2007.321.
[51] T.G. Lucas, B.J. Henriques, J.V. Rodrigues, P. Bross, N. Gregersen, C.M. Gomes, Cofactors and metabolites as potential stabilizers of mitochondrial acyl-CoA dehydrogenases, Biochim. Biophys. Acta 2011 (1812) 1658–1663, https://doi.org/10.1016/j.bbadis.2011.09.009.
[52] D. Matulis, J.K. Kranz, F.R. Salemme, M.J. Todd, Thermodynamic stability of carbonic anhydrase: measurements of binding affinity and stoichiometry using ThermoFluor, Biochemistry 44 (2005) 5258–5266, https://doi.org/10.1021/bi048135v.

[53] J. Zeng, D. Li, Expression and purification of His-tagged rat mitochondrial medium-chain acyl-CoA dehydrogenase wild-type and Arg256 mutant proteins, Protein Expr. Purif. 37 (2004) 472–478, https://doi.org/10.1016/j.pep.2004.06.021.
[54] R. Ghosh, J.R. Quayle, Phenazine ethosulfate as a preferred electron acceptor to phenazine methosulfate in dye-linked enzyme assays, Anal. Biochem. 99 (1979) 112–117, https://doi.org/10.1016/0003-2697(79)90050-2.
[55] G.A. Senisterra, B. Soo Hong, H.W. Park, M. Vedadi, Application of high-throughput isothermal denaturation to assess protein stability and screen for ligands, J. Biomol. Screen. 13 (2008) 337–342, https://doi.org/10.1177/1087057108317825.
[56] A.P. Pandurangan, B. Ochoa-Montano, D.B. Ascher, T.L. Blundell, SDM: a server for predicting effects of mutations on protein stability, Nucleic Acids Res. 45 (2017) W229–W235, https://doi.org/10.1093/nar/gkx439.
[57] E.F. Pettersen, T.D. Goddard, C.C. Huang, G.S. Couch, D.M. Greenblatt, E.C. Meng, T.E. Ferrin, UCSF Chimera—a visualization system for exploratory research and analysis, J. Comput. Chem. 25 (2004) 1605–1612, https://doi.org/10.1002/jcc.20084.
[58] L.P. O'Reilly, B.S. Andresen, P.C. Engel, Two novel variants of human medium chain acyl-CoA dehydrogenase (MCAD). K364R, a folding mutation, and R256T, a catalytic-site mutation resulting in a well-folded but totally inactive protein, FEBS J. 272 (2005) 4549–4557, https://doi.org/10.1111/j.1742-4658.2005.04878.x.
[59] Y. Ikeda, K. Okamura-Ikeda, K. Tanaka, Purification and characterization of short-chain, medium-chain, and long-chain acyl-CoA dehydrogenases from rat liver mitochondria. Isolation of the holo- and apoenzymes and conversion of the apoenzyme to the holoenzyme, J. Biol. Chem. 260 (1985) 1311–1325.
[60] C.A. Bonito, P. Leandro, F.V. Ventura, R.C. Guedes, Insights into medium-chain acyl-CoA dehydrogenase structure by molecular dynamics simulations, Chem. Biol. Drug Des. 88 (2016) 281–292, https://doi.org/10.1111/cbdd.12755.
[61] S.W. Gersting, K.F. Kemter, M. Staudigl, D.D. Messing, M.K. Danecka, F.B. Lagler, C.P. Sommerhoff, A.A. Roscher, A.C. Muntau, Loss of function in phenylketonuria is caused by impaired molecular motions and conformational instability, Am. J. Hum. Genet. 83 (2008) 5–17, https://doi.org/10.1016/j.ajhg.2008.05.013.
[62] C.S. Tome, R.R. Lopes, P.M.F. Sousa, M.P. Amaro, J. Leandro, H.D.T. Mertens, P. Leandro, J.B. Vicente, Structure of full-length wild-type human phenylalanine hydroxylase by small angle X-ray scattering reveals substrate-induced conformational stability, Sci. Rep. 9 (2019) 13615, https://doi.org/10.1038/s41598-019-49944-x.
[63] H. Pavlu-Pereira, D. Lousa, C.S. Tome, C. Florindo, M.J. Silva, I.T. de Almeida, P. Leandro, I. Rivera, J.B. Vicente, Structural and functional impact of clinically relevant E1alpha variants causing pyruvate dehydrogenase complex deficiency, Biochimie 183 (2021) 78–88, https://doi.org/10.1016/j.biochi.2021.02.007.
[64] M. Staudigl, S.W. Gersting, M.K. Danecka, D.D. Messing, M. Woidy, D. Pinkas, K. F. Kemter, N. Blau, A.C. Muntau, The interplay between genotype, metabolic state and cofactor treatment governs phenylalanine hydroxylase function and drug response, Hum. Mol. Genet. 20 (2011) 2628–2641, https://doi.org/10.1093/hmg/ddr165.
[65] L. O'Reilly, P. Bross, T.J. Corydon, S.E. Olpin, J. Hansen, J.M. Kenney, S. E. McCandless, D.M. Frazier, V. Winter, N. Gregersen, P.C. Engel, B.S. Andresen, The Y42H mutation in medium-chain acyl-CoA dehydrogenase, which is prevalent in babies identified by MS/MS-based newborn screening, is temperature sensitive, Eur. J. Biochem. 271 (2004) 4053–4063, https://doi.org/10.1111/j.1432-1033.2004.04343.x.
[66] S. Mosegaard, G. Dipace, P. Bross, J. Carlsen, N. Gregersen, R.K.J. Olsen, Riboflavin deficiency-implications for general human health and inborn errors of metabolism, Int. J. Mol. Sci. 21 (2020), https://doi.org/10.3390/ijms21113847.
[67] M. Duran, C.B. Cleutjens, D. Ketting, L. Dorland, J.B. de Klerk, F.J. van Sprang, R. Berger, Diagnosis of medium-chain acyl-CoA dehydrogenase deficiency in lymphocytes and liver by a gas chromatographic method: the effect of oral riboflavin supplementation, Pediatr. Res. 31 (1992) 39–42, https://doi.org/10.1203/00006450-199201000-00007.
[68] T.G. Derks, C.M. Touw, G.S. Ribas, G.B. Biancini, C.S. Vanzin, G. Negretto, C. P. Mescka, D.J. Reijngoud, G.P. Smit, M. Wajner, C.R. Vargas, Experimental evidence for protein oxidative damage and altered antioxidant defense in patients with medium-chain acyl-CoA dehydrogenase deficiency, J. Inherit. Metab. Dis. 37 (2014) 783–789, https://doi.org/10.1007/s10545-014-9700-0.